Electron Affinities and Electron-Transfer Reactions

PAUL KEBARLE* and SWAPAN CHOWDHURY

Chemistry Department, University of Alberta, Edmonton, Alberta, Canada, T6G 2G2

Received January 8, 1987 (Revised Manuscript Received February 17, 1987)

Contents

Paul Kebarle was born in Sofia, Bulgaria. He studied chemistry at ETH in Zurich, Switzerland, and took his Ph.D. in Physical Chemistry (reaction kinetics) at the University of British Columbia in Vancouver. After 2 years postdoctoral work with Fred Lossing at NRC Ottawa he joined the academic staff at the Chemistry Department of the University of Alberta in 1958. Studies of ions in gases near atmospheric pressures in his laboratory in 1964 led to the discovery that ion–molecule equilibria occur spontaneously at higher pressures and can be measured under these conditions. His research since that time has been devoted to the study of ion–molecule reaction equilibria and the application of the data in various areas of chemistry.

Swapan Chowdhury was born in Chittagong, Bangladesh. He obtained his B. Sc. (Honors) and M. Sc. degrees in Chemistry from the University of Chittagong. Very recently he received his Ph.D. degree from the University of Alberta, where he worked under the direction of Professor Paul Kebarle. Currently he is doing postdoctoral research, involving tendem mass spectrometry, with Professor Alex. Harrison at the University of Toronto. His research interests are in the general area of mass spectrometry with special emphasis on analytical techniques, such as chemical ionization (CI), collision-induced dissociation (CID), and fast-atom bombardment (FAB).

I. Introduction

The electron affinities of molecules are of interest not only in areas where gas-phase ions are encountered, e.g., negative-ion analytical mass spectrometry,[1–5] gas-phase radiation chemistry,[6] ionosphere,[7] gaseous electronics,[8] electron capture detector gas chromatography,[9–11] and gas-phase ion chemistry,[12] but also in the much wider field of condensed-phase chemistry. Charge-transfer complexes and their role in organic, biological, and catalytic processes represent an example of a vast condensed-phase area for which knowledge of electron affinities is of prime importance.[16–18] Even more important is the role of electron transfer in biological redox processes.[13] Rich,[13] Christophorou,[14] Szwarc,[15] and Biergleb[16] have discussed the significance of electron affinity to these areas. Eberson[17] has recently considered the possible relationships between dissociative electron transfer and toxicity of the compounds involved in dissociative electron transfer. Single-electron-transfer reactions in solution belong to a major research area in inorganic chemistry.[18] Reductions through single-electron transfer from alkali metals to unsaturated organic compounds, e.g., Bouveault–Blanc and Birch reductions, have been of importance in synthetic organic chemistry for a number of years. Furthermore, some reactions that were previously consid-

0009-2665/87/0787-0513$06.50/0

ered to be of the S_N2 type have now been reinterpreted on the basis of single-electron-transfer mechanisms.[19] In all these solution reactions, the stabilities of the anions are of prime importance, and these depend on the gas-phase electron affinity and on the solvation energy of the anion.

Since the electron affinity (EA) is such an important fundamental property, it is not surprising that many methods for EA determination have been used. Thus in a 220-page recent review of electron affinities by Christophorou,[20] some 31 different methods for electron affinity determinations are described. In spite of the availability of a large number of methods and the fundamental importance of EA values, data are not available for many molecules of interest,[20] and when data are available, there can be very significant disagreement between different determinations.[20]

Two other recent reviews of electron affinities are by Lineberger[21] and Brauman[22] (see also papers by these authors in this issue). The electron photodetachment studies described by these authors represent the most accurate methods for EA determination. For diatomic and small polyatomic molecules where the photodetachment spectrum can be resolved, i.e., where the initial and final states involved in the transitions can be identified, one obtains not only EA but also vibrational spacings in the neutral molecule and the negative ion. However, when polyatomic molecules are involved and the geometry of the negative ion and the neutral are quite different, resolution of the spectra may be difficult. The problem may be further aggravated when internal excitation is present in the negative ion (hot bands). The photodetachment spectrum in such cases may be so complicated that an electron affinity determination cannot be obtained.

Gas-phase ion–molecule equilibria measurements, first developed and demonstrated in this laboratory[23,24] with a pulsed electron high ion source pressure mass spectrometer (PHPMS) (see Figures 1 and 2) and later also executed in an ion cyclotron[25] and flowing afterglow appratuses,[26] have proven to be an extraordinarily prolific source of ion thermochemical data such as ion–ligand binding energies,[24,27] proton affinities of neutrals (gas-phase basicities) and negative ions (gas-phase acidities),[28,29] and hydride and chloride affinities of carbocations.[30]

Relative electron affinities can also be determined with the ion–molecule equilibrium technique. The equilibria involved are given in eq 1.

$$A^- + B = A + B^- \quad (1)$$

$$K_1 = \frac{[B^-][A]}{[A^-][B]} \quad (2)$$

$$\Delta G_1^\circ = -RT \ln K_1 = \Delta H_1^\circ - T\Delta S_1^\circ \quad (3)$$

$$e + B = B^- \quad (4)$$

$$\Delta H_4^\circ = \Delta H_a^\circ(B) \qquad \Delta G_4^\circ = \Delta G_a^\circ(B) \quad (5)$$

$$\Delta H_1^\circ = \Delta H_a^\circ(B) - \Delta H_a^\circ(A) \quad (6)$$

$$-EA(B) \approx \Delta H_a^\circ(B) \quad (7)$$

The equilibrium constant K_1, given in eq 2, is determined by the experimental measurement. One obtains the electron-transfer free energy ΔG_1° from eq 3. The corresponding enthalpy can be obtained via van't Hoff plots of K_1 measured at different temperatures or from extrathermodynamic estimates of ΔS_1°, the entropy changes, which are generally quite small. A series of interconnected equilibria is measured such that a continuous ΔG_1° and ΔH_1° scale (ladder) is obtained. Absolute electron affinities (eq 4–6) are obtained by calibrating the scale to the known, literature, electron affinity of one or more of the participating compounds. These compounds are the external standards or "anchors" of the scale. The technique and procedures are described in more detail in section II of this article.

Fukuda and McIver,[31-34] using a pulsed ICR, were the first investigators to measure equilibria 1. The compounds A and B involved were mostly singlet molecules such that electron capture led to doublet radical anions. Unfortunately, due to a faulty determination of the EA of SO_2 and nitrobenzene,[32] these authors anchored the electron affinity scale incorrectly.[35,36] Extensive measurements of equilibria 1 from the reviewers' laboratory were initiated in 1983. The method proved to be very efficient and relatively straightforward. This allowed the determination of the electron affinities of some 120 compounds up to the present time.[36-47]

All compounds involved were stable molecules with positive electron affinities. The vast majority were singlet molecules which on electron capture became radical anions.

The measurement of the electron-transfer equilibria (ETE) almost automatically leads also to a study of the kinetics of the electron-transfer reactions (eq 1). The rate constants of some 90 electron-transfer reactions were determined.[37-43,45,46] Exothermic ion–molecule reactions in the gas phase often proceed at collision rates, and this was found also to be the case for electron transfer. Collision rate constants provide little information on the details of the electron-transfer process. More interesting are exothermic electron-transfer reactions which proceed with rates that are lower than collision rates. The slow rates generally reveal the magnitude of the energy barrier for the electron-transfer process. The kinetic results and discussion are given in section III of this paper.

Typically, organic compounds with positive electron affinities possess conjugated bonds, and this leads to a relatively low-lying lowest unoccupied molecular (π^*) orbital (LUMO), which accepts the extra electron and becomes the singly occupied molecular orbital (SOMO). In addition to conjugation, the presence of electronegative atoms or electron-withdrawing groups (F, Cl, CHO, CN, NO_2) leads to lowering of the LUMO energy and thus to a higher electron affinity. The compounds whose EA's were determined were substituted benzenes, naphthalenes, anthracenes, substituted quinones, perfluorinated systems like C_6F_6 and SF_6, perfluorocycloalkanes, and some smaller molecules like SO_2, NO_2, and CH_3NO_2.

The results of the electron affinity determinations and relationships between structure and stability of the anions are examined in section IV of this paper.

The measured entropy changes on electron attachment ΔS_a° can in certain cases provide useful information on the structural changes occurring on formation of the negative ion. These results are discussed in section V.

The electron-transfer reactions in the gas phase may proceed via relatively long-lived adduct complexes $A^-\cdot B$. In some cases the adduct complexes can be stabilized by collisions with a third gas, and the equilibria (eq 8) can be measured.

$$A^- + B = A^-\cdot B \quad (8)$$

Such measurements lead to determinations of the binding energies $\Delta G_8°$ and enthalpies $\Delta H_8°$ of the adduct $A^-\cdot B$. The binding energies may indicate characteristic binding between the anion and the molecule, i.e., hydrogen bonding or covalent bonding as in Meisenheimer complexes. Furthermore, the bonding in $A^-\cdot B$ may be of importance to the kinetics of the electron-transfer reaction. These results and discussion are given in section VI.

As mentioned above, radical anions are important species in solution. The available gas-phase electron affinities can be compared with energy data in solution. Most useful in this respect are the polarographic half-wave reduction potentials $E_{1/2}$. Combination of the gas-phase data with the solution reduction potentials leads to evaluations of the solvation energies of the radical anions. Additional insight into the nature of the solvation interactions can be obtained by measurement of the gas-phase ion–molecule equilibria 9, where B^- is

$$B^- + Sl = B^-\cdot Sl \qquad B^-(Sl)_{n-1} + Sl = B^-(Sl)_n \quad (9)$$

a given anion and Sl is a molecule of a solvent vapor like methanol, acetonitrile, or dimethylformamide. These data and discussion are also presented in section VI of this paper.

The formation of negative ions B^- in the presence of B and thermal electrons depends on the temperature and pressure and the internal properties of B and B^-. More directly, the observation of B^- depends on the values of the electron thermal attachment and detachment rate constants. These relationships are discussed in section VII.

Negative ions play an important part in analytical mass spectrometry. Particularly important areas are chemical ionization (NICI), fast atom bombardment (NIFAB), thermospray, and electrospray. The relevance of the PHPMS results to these fields is discussed in section VIII.

The literature coverage in this article restricts itself to gas-phase electron-transfer reactions and equilibria and electron affinities derived therefrom. Most of this work is contained in ref 31–47. Other literature is covered only insofar as it relates to the data obtained from electron-transfer equilibria and the kinetics studies. The literature coverage extends to September 1986.

II. Determination of Electron-Transfer Equilibria (ETE) and Electron Affinities (EAs)

The electron-transfer equilibria (eq 1) were measured in the laboratory of the reviewers with the pulsed electron beam high ion source pressure mass spectrometer[48] (PHPMS) used in earlier work.[24] The pulsed electron, ion source (see Figure 1) contains typically 5 Torr of bath gas, most often methane, and millitorr pressures of compounds A and B. A short ~10-μs pulse of electrons accelerated by 2000 V enters the ion source through a very narrow slit and leads to production of

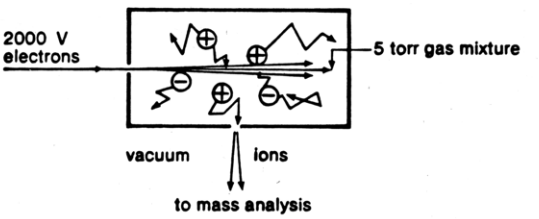

Figure 1. Ion source of pulsed electron high pressure mass spectrometer PHPMS. Relatively high bath gas pressure (5 Torr) traps ions since it slows diffusion of ions to walls. Also, high bath gas pressure leads to *thermal* reaction conditions.

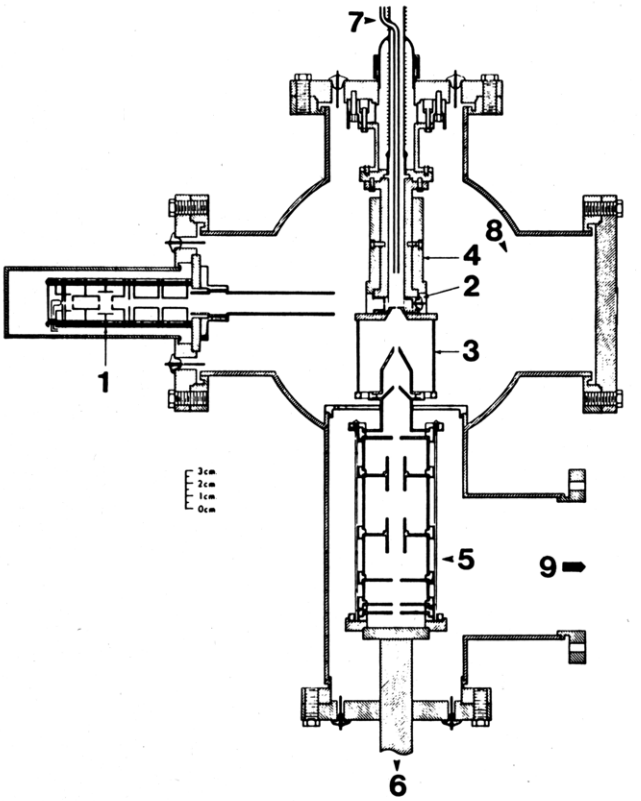

Figure 2. PHPMS apparatus: (1) pulsed electron gun: (2) temperature-controlled ion source; (3) open cage defining electrical field; (4) heating and cooling mantle; (5) accelerating electrodes; (6) to magnetic mass analysis tube; (7) slow in and out flow of reaction mixture through ion source; (8) 6-in. differential pumping; (9) 4-in. differential pumping.

positive ions and secondary electrons by electron impact with the bath gas. The secondary electrons are brought to near thermal energies by collisions with the bath gas. Electron capture by A and B leads to excited $(A^-)^*$ and $(B^-)^*$, which are subsequently thermalized by collisions with the bath gas. As A^- and B^- diffuse toward the walls they engage also in electron transfer with neutral B and A molecules, and the electron-transfer equilibrium (eq 1) is achieved under suitably selected conditions. The ions coming to the vicinity of the very narrow ion exit slit escape into the vacuum chamber where they are accelerated, mass analyzed, and detected (see Figure 2). The time between pulses is typically 10 ms. One given mass is observed over some 5000–10 000 pulses, the accumulated signal leading to better signal-to-noise ratio. The ions arriving at the ion detector after the electron pulse are counted and the counts stored in a multiscaler as a function of time.[48] Ion intensities obtained in typical experiments[37] are shown in Figure 3. Electron capture by A and B leads

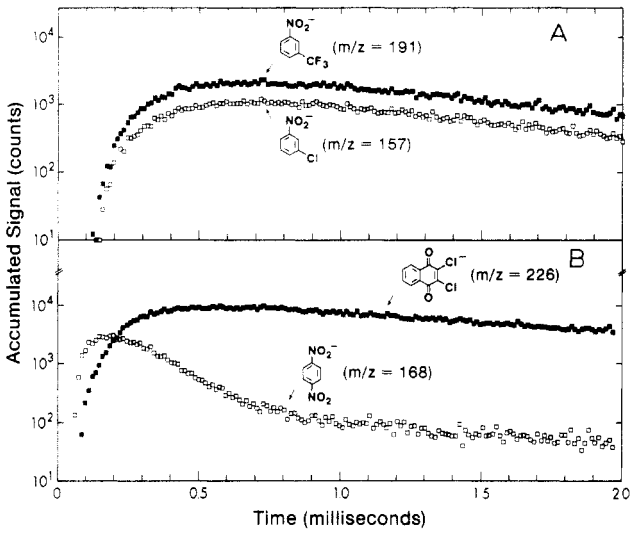

Figure 3. Observed[37] ion intensities after 10-μs electron pulse. In B, a kinetic stage precedes achievement of electron-transfer equilibrium, while in A the equilibrium is established rapidly.

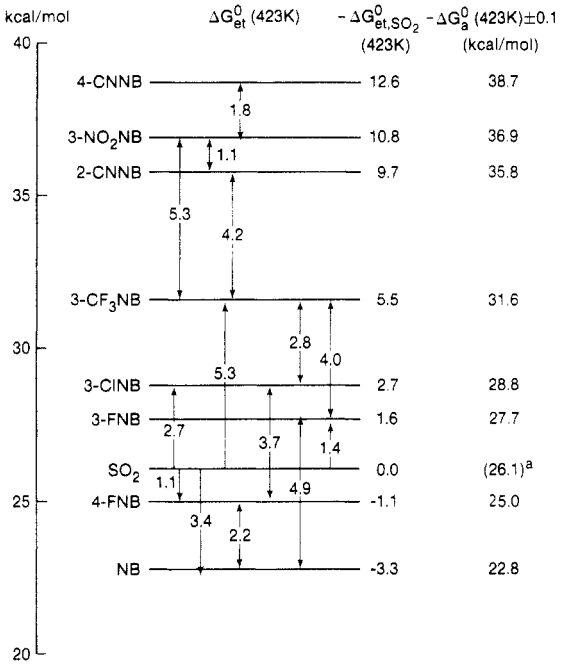

Figure 4. Partial ladder (scale) giving values for $\Delta G_1° = \Delta G_{et}$ for the electron-transfer equilibria $A^- + B = A + B^-$. These $\Delta G°$ values can be combined to provide $\Delta G_{et}°(SO_2)$ for the reaction $SO_2^- + A = SO_2 + A^-$. Known $\Delta G_a°(SO_2) = -26.1$ kcal/mol evaluated from literature data leads to $\Delta G_a°(A)$ for all of the other compounds. $\Delta G_a°(A)$ corresponds to the reaction $A + e = A^-$. Scale illustrates connections to the standard SO_2. NB stands for nitrobenzene. The subscript a in $\Delta G_a°$ stands for attachment process (eq 4).

to formation of A^- and B^- (Figure 3B). However, due to the higher electron affinity of the dichloronaphthoquinone (B), the intensity of B^- is seen to increase with time while that of A^- decreases. After some 0.7 ms, the intensity ratio B^- to A^- becomes constant with time, which for the logarithmic intensity plot used corresponds to a constant vertical distance between B^- and A^-. The constant ratio is assumed to be due to achievement of equilibrium 1. In Figure 3A conditions are such that the equilibrium is established much faster. In both A and B the linear decrease of the log ion intensities after equilibrium has been reached is due to first-order diffusion and destruction of the ions at the

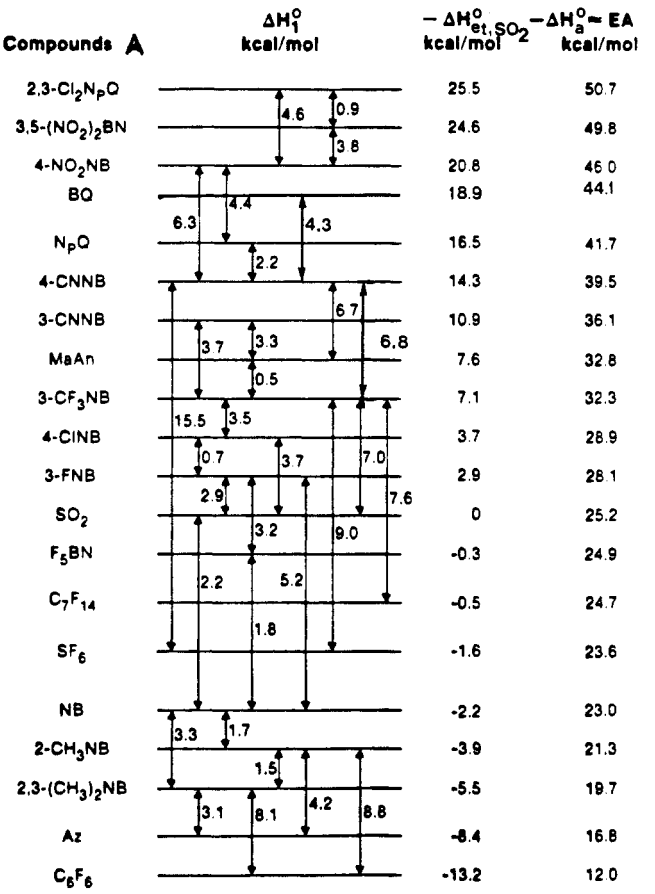

Figure 5. Partial $\Delta H_1°$ scale based on van't Hoff plots of equilibrium constants K_1 for electron-transfer reaction 1: $A^- + B = A + B^-$. Also given are $\Delta H_{et}(SO_2)$ values corresponding to ΔH for the reaction $SO_2^- + A = SO_2 + A^-$. Absolute ΔH_a corresponding to $e + A = A^-$ are obtained by calibration to literature $EA(SO_2)$. From Chowdhury.[41]

wall of the ion source. The ion intensity ratio after equilibrium is achieved is substituted into the equilibrium constant equation (eq 2). The concentrations of the neutrals A and B are known from the original composition of the mixture. Ion formation is a minor process, so that [A] and [B] remain virtually unchanged.

A ladder (scale) constructed from $\Delta G_1°$ values obtained from some of the electron-transfer equilibria measurements[37-46] is shown in Figure 4. Determinations of K_1 at different temperatures lead to the evaluation of $\Delta H_1°$ and $\Delta S_1°$ via van't Hoff plots (see eq 2 and 3). Thus, one can also construct $\Delta H_1°$ and $\Delta S_1°$ ladders.[41-45] Partial $\Delta H_1°$ and $\Delta S_1°$ ladders are given in Figures 5 and 6. The electron affinities of the compounds in the $\Delta H_1°$ ladder are evaluated[41] from the electron affinity of SO_2 determined with the electron photodetachment method by Hall.[49] Furthermore, there are four[50-53] other electron affinity values for $SO_{2(g)}$ within ±0.1 eV of Hall's value: 1.097 ± 0.036 eV. SO_2 is a good standard also because the geometries and vibrational frequencies of SO_2 and SO_2^- are available from the literature (see Table I, ref 41).

The photodetachment electron affinity[49] corresponds to the negative energy change for the electron attachment process (eq 10) where SO_2 and SO_2^- are in their

$$SO_2 + e = SO_2^- \qquad \Delta H_a(SO_2) \qquad (10)$$

ground electronic, vibrational, and rotational states. By use of the stationary convention for the electron,[41]

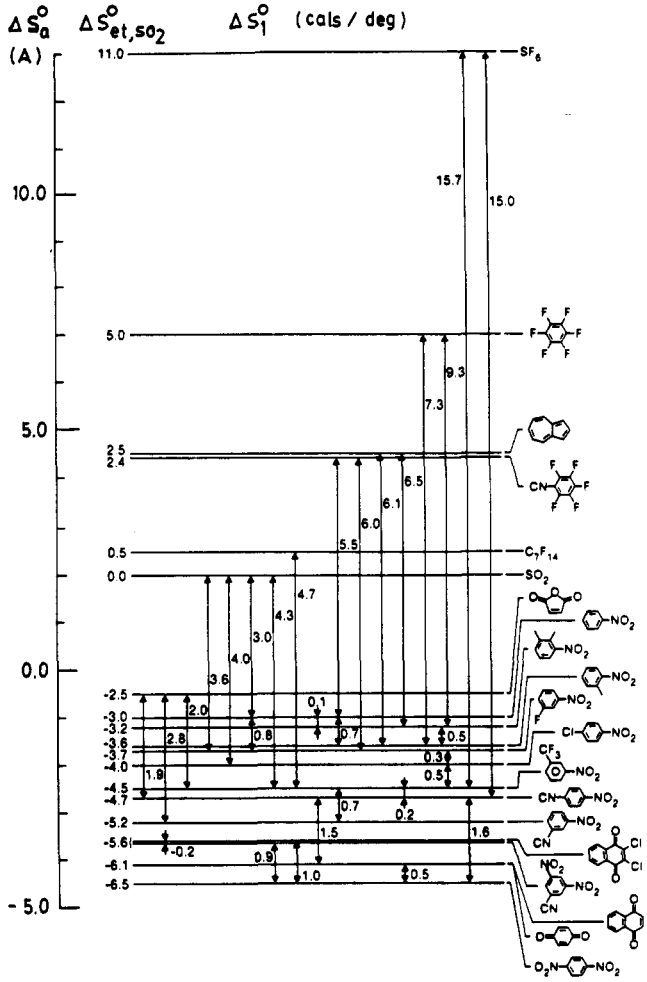

Figure 6. Partial $\Delta S_1°$ scale based on van't Hoff plots of equilibrium constants K_1 for the reactions $A^- + B = A + B^-$. From these, $\Delta S_{et}°(SO_2)$ corresponding to the reaction $SO_2^- + A = SO_2 + A^-$ is derived. $\Delta S_a°$ corresponding to the reaction $A + e = A^-$ is derived from literature data for $\Delta S_a(SO_2)$. From Chowdhury.[41] Subscript a stands for attachment process (eq 4).

$EA(SO_2)$ corresponds to the $-\Delta H_a(SO_2)$ at 0 K. $\Delta H_a(SO_2)$ at 298 K can be evaluated[41] from the available vibrational frequencies of SO_2 and SO_2^- and $EA(SO_2)$.[49] Due to the similarities of SO_2 and SO_2^-, $\Delta H_a°$ at 298 and 0 K are found to differ by only 0.1 kcal/mol, a difference that is smaller than the expected error of the $\Delta H_1°$ measurements.

$$\Delta H_a(SO_2)_{298} = -EA(SO_2) + 0.1 \text{ kcal/mol}$$

Electron attachment entropies for SO_2^-, $\Delta S_a°(SO_2)$, can also be evaluated from the available frequencies and geometries.[41] Thus SO_2 serves also as an anchor in the entropy as well as free energy ladder (see Figures 4–6).

III. Kinetics of Electron-Transfer Reactions 1: $A^- + B = A + B^-$

Electron transfer (1) involving negative ions in its essential features is analogous to electron transfer involving positive ions (eq 11). Reactions 1 or 11 are

$$A^+ + B = A + B^+ \qquad (11)$$

often referred to as charge-transfer reactions by workers in the gas phase. Electron-transfer reactions have been much studied both in the gas phase and in solution.[18,19]

Early theoretical work involving gaseous atomic ions and neutral atoms dealt with the velocity dependence of the electron-transfer cross section.[54,55] This work established that the conversion of translational energy into internal (electronic) energy is a relatively inefficient process. The largest cross sections are occurring for resonant processes, i.e., for cases where the recombination energy of A^+ matched the ionization energy of B, at near zero relative velocities. For brief reviews see Futrell[56] and Lindholm.[57]

Early qualitative extensions of the theory based on experimental findings for diatomic systems and thermal rate constants were published by Bohme[58] and Bowers.[59] These and earlier authors emphasized the importance of "accidental" resonance for molecular systems. Accidental resonance is achieved by transitions to electronically and vibrationally excited states whose density might be quite high for molecules. Since the transition from $A^+ \cdot B$ to $A \cdot B^+$ involves a fast electron jump, the transitions are vertical, i.e., the internuclear distances in the molecules A and molecules B are, from a classical view point, preserved, or, quantum mechanically, the transition probability is governed by the Franck–Condon factors. Implicit in these treatments is also the assumption of weak electronic overlap between A^+ and B in $A^+ \cdot B$ and A and B^+ in $A \cdot B^+$, where $A^+ \cdot B$ and $A \cdot B^+$ are the complexes just before and after the electron jump.

A systematic experimental and theoretical development concerning the rate constants of electron-transfer reactions involving polyatomic molecules does not seem to have occurred. For a brief discussion and leading references see the Introduction in McEwen.[60] It has been recognized that for electron-transfer reactions the classical spiralling collision rate constant (Langevin-ADO)[61,62] need not be the upper limit. In cases where energy resonance is present and the Franck–Condon factors are very favorable, the electron jump may occur in the "fly by" at distances larger than those corresponding to the classical orbiting limit, although firm experimental evidence for the occurrences of such large rate constants does not seem to be available.[60] The majority of thermal exothermic electron-transfer reactions involving polyatomic reactants occur at near collision limit rates.

Relatively few determinations of thermal rate constants for the electron-transfer reactions (eq 1) involving negative ions have been reported.[7,35,60,63–65] Most of these studies[7,35,63–65] were performed primarily for the determination of electron affinities via (1), where, instead of measuring the equilibrium (eq 1), one measures rates (bracketing method). The assumption is made that if the reaction is exothermic it will proceed at near collision rates.[65]

Systematic determinations of thermal rate constants k_1 were undertaken in the reviewers' laboratory from 1984 onward.[37,38,40,42–46] A description of the method of measurement is given in Grimsrud.[37] Some 90 rate constants were determined. Part of these are summarized in Table I.

Exothermic electron transfer between NO_2, SO_2, substituted benzenes, perfluoroaromatics, quinones, naphthalenes, anthracenes, and azulene was found to proceed at near collision rates. In most cases (see Table IA), the rate constants predicted by ADO theory[62] were found to be in good agreement with the experimental determinations.

TABLE I

(A). Rate Constants for Exothermic Electron-Transfer Reactions 1: $A^- + B = A + B^-$

	A[a]	B[a]	k_1(exptl)[b]	k_1(ADO)[c]		A[a]	B[a]	k_1(exptl)[b]	k_1(ADO)[c]
1	NB	p-NO_2NB	1.3	1.1	11	p-NO_2NB	NO_2	0.4	0.6
2	NB	m-NO_2NB	2.1	1.8	12	BQ	NO_2	0.3	0.5
3	m-CF_3NB	p-NO_2NB	1.3	1.0	13	azulene	m-CF_3NB	1.0	
4	p-FNB	m-NO_2NB	1.9	1.8	14	p-FNB	BQ	1.4	
5	NB	m-CF_3NB	1.8	1.8	15	p-NO_2NB	2,6-Cl_2BQ	1.0	
6	p-MeNB	m-Cf_3NB	1.9	1.7	16	p-NO_2NB	2,3-Cl_2NpQ	0.4	
7	NB	NO_2	0.4	0.6	17	2,3-Cl_2NpQ	2,6-Cl_2BQ	1.5	
8	p-CH_3NB	NO_2	0.5	0.6	18	2,6-Cl_2BQ	Cl_4BQ	0.5	
9	p-ClNB	NO_2	0.5	0.6	19	C_7F_{14}	2,6-Cl_2BQ	0.8	
10	m-NO_2NB	NO_2	0.5	0.6	20	C_7F_{14}	NO_2	0.08	

(B). Exothermic Electron Transfer Rate Constants k for $A^- + B \rightarrow A + B^-$ Involving SF_6 and C_7F_{14} at 423 K

A	B	$-\Delta H°$	k(obsd)[e,f]	E_v[g]	$E^{\ddagger}$[h]
SF_6	3-$CF_3C_6H_4NO_2$	8.9	5×10^{-13}	6.9	7.4
SF_6	3-$NO_2C_6H_4NO_2$	14.5	6×10^{-11}	6.0	5.4
SF_6	4-$CNC_6H_4NO_2$	15.5	1.0×10^{-10}	4.3	4.8
SF_6	4-$NO_2C_6H_4NO_2$	22.5	1.0×10^{-9}	3.0	2.9
SF_6	$F_4C_6O_2$	38.6	1.4×10^{-9}	0.0	0.3
$CF_3C_6F_{11}$	3-$CF_3C_6H_4NO_2$	7.7	$<5 \times 10^{-13}$		
$CF_3C_6F_{11}$	3-$NO_2C_6H_4NO_2$	13.3	4×10^{-11}		
$CF_3C_6F_{11}$	4-$CNC_6H_4NO_2$	14.6	5×10^{-11}		
$CF_3C_6F_{11}$	4-$NO_2C_6H_4NO_2$	21.3	7×10^{-10}		
$CF_3C_6F_{11}$	2,6-$Cl_2C_6H_2O_2$	32.3	8×10^{-10}		
$CF_3C_6F_{11}$	$F_4C_6O_2$	37.4	1.2×10^{-9}		

[a] NB = nitrobenzene; BQ = p-benzoquinone; NpQ = 1,4-naphthoquinone; C_7F_{14} = perfluoromethylcyclohexane. [b] (cm^3 $molecule^{-1}$ s^{-1}) × 10^9. [c] (cm^3 $molecule^{-1}$ s^{-1}) × 10^9. The following dipole moments (in Debye) and polarizabilities (in Å^3) were used: p-NO_2NB, 0, 15.5; m-NO_2NB, 3.8, 15.5; m-CF_3NB, 3.6, 18; NO_2, 0.3, 2.5. For ADO equations see Bowers.[79] [d] In kcal/mol. [e] Rate constants in cm^3 $molecule^{-1}$ s^{-1}. [f] From ref 38. [g] E_v equals vibrational energy in kcal/mol in SF_6^- present in complex SF_6^-·B required for $E_{d,v}$ = EA(B) (see Figure 9). [h] $E^{\ddagger}$ in kcal/mol is calculated by Richardson[71] on the basis of the Marcus equations.

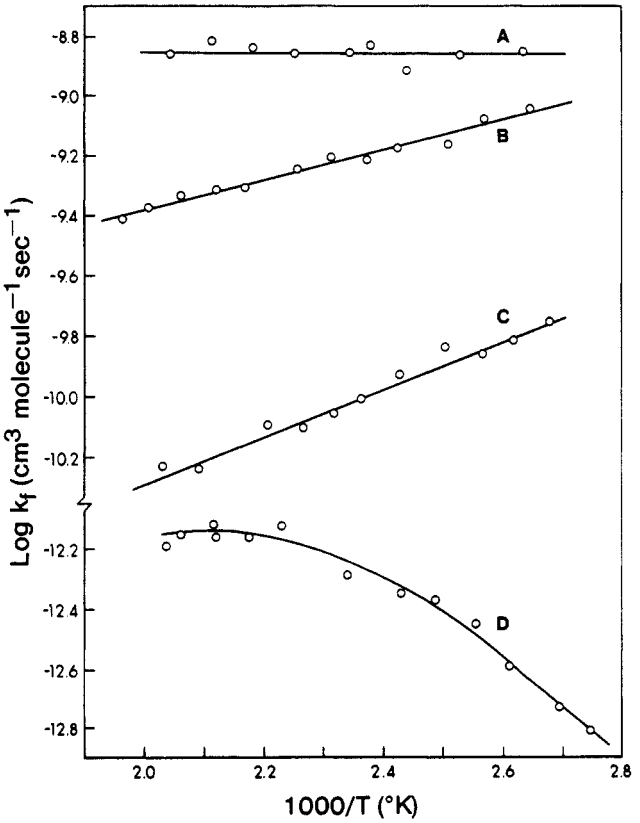

Figure 7. Temperature dependence of forward rate constant, k_f, for slow reactions 12: $SF_6^- + B = SF_6 + B^-$: (A) B = tetrafluoroquinone; (B) B = 1,4-dinitrobenzene; (C) B = 4-cyano-1-nitrobenzene; (D) B = 3-(trifluoromethyl)-1-nitrobenzene. EA(B) decreases from A to D. Rate constant decreases in same order. From Grimsrud.[38]

Rates much slower than collision rates were observed[38] for SF_6, perfluorocyclohexane, and perfluoromethylcyclohexane. The rate constants for these slow reactions are given in Table IB. More detailed information was obtained for reaction 12, where B were

$$SF_6^- + B = SF_6 + B^- \qquad (12)$$

nitrobenzenes or quinones with differing electron affinities such that the exothermicity of (12) could be changed by small increments. The temperature dependence of the rate constants k_{12} for four different B's was determined. These results[38] are shown in Figure 7.

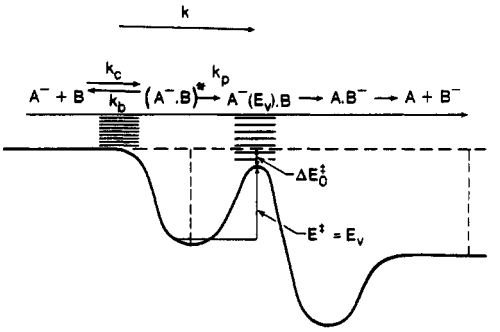

Figure 8. Typicl reaction coordinate for bimolecular ion–molecule reactions. Internal barrier, $E^{\ddagger}$, becomes equal to the vibrational energy, E_v, shown in Figure 9 for the special case of electron-transfer reactions 12: $SF_6^- + B = SF_6 + Br^-$. From Grimsrud.[38]

Rate constants of ion–molecule reactions proceeding at collision rates do not provide information on the nature of the chemical transition state via which the actual transforming event occurs since they depend on the parameters of the bottleneck complex, which in this case is the orbiting complex. The typical reaction coordinate[66,67] for ion–molecule reactions is shown in Figure 8. Initially, the energy decreases due to the long-range attractive forces between the ion and in-

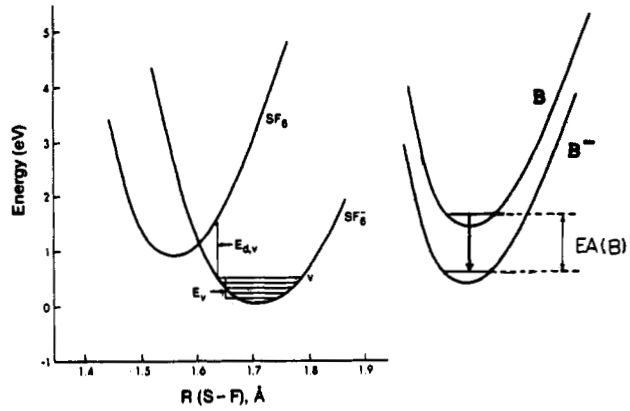

Figure 9. Potential energies of SF_6 and SF_6^- from theoretical calculations of Hay.[70] Assuming negligible geometry change between B and B^-, conservation of energy leads to the requirement $EA(B) \approx E_{d,v}$, which fixes the value of internal barrier E_v for electron transfer (eq 12). See Figure 8.

duced plus permanent dipoles of the molecule. When the chemical barrier $E^{\ddagger}$ is low such that $-\Delta E_0^{\ddagger}$ is large, formation of the collision complex is rate determining; i.e., $k = k_c$ and no information on $-\Delta E_0^{\ddagger}$ apart from an (approximate) upper limit is obtained from k. Since k_c is almost independent of temperature,[61,62] these reactions show weak or no temperature dependence.

For reactions in which the chemical barrier is relatively larger such that $\Delta E_0^{\ddagger}$ is still negative but $-\Delta E_0^{\ddagger}$ is small, passage over this barrier becomes rate determining. k is less than k_c and increases as the temperature is decreased; i.e., there is negative temperature dependence. For relatively large $E^{\ddagger}$ where $\Delta E_0^{\ddagger}$ is positive, k is very much smaller than k_c and has positive temperature dependence.[66,67]

The above findings[66,67] were based on studies of ion–molecule reactions where the chemical transformation occurs through continuous nuclear motion. This is the case, for example, in S_N2 reactions. Electron-transfer reactions are special since the "chemical transformation" occurs with an electron jump at some constant atomic coordinates (Franck–Condon transition). An internal energy barrier $E^{\ddagger}$ for electron-transfer reactions can be present when the geometries of $A^-\cdot B$ and $A\cdot B^-$ are quite different.[68] Since electron transfer among the compounds B, which were the nitrobenzenes, quinones, etc., was fast, Grimsrud et al.[38] concluded that the big change between $SF_6^-\cdot B$ and $SF_6\cdot B^-$ in the slow reactions (eq 12) occurs in the geometries of SF_6^- and SF_6. This assumption was supported by experimental observations[69] on the photodetachment threshold of SF_6^- and a theoretical calculation by Hay,[70] which showed that the S–F bonds in SF_6^- were considerably longer than in SF_6. Hay's result is shown in Figure 9. Making the assumption that $E_{d,v} \approx EA(B)$, which is equivalent to the requirement that the $A^-\cdot B \rightarrow A\cdot B^-$ transformation should conserve internal energy, Grimsrud et al.[68] obtained the vibrational energy $E_v = E^{\ddagger}$. E_v is the vibrational energy in SF_6^- required for a good Franck–Condon probability (see Figure 9). These $E^{\ddagger}$ are given in Table IB. The approach taken by Grimsrud et al.[38] corresponds to a graphical solution of the Marcus equations,[18,68] although the authors[38] were not aware of this at the time. Later, Richardson,[71] using the assumption of similar geometries for B and B^- and Hay's potential energies for SF_6 and SF_6^-, evaluated the barriers for reactions 12 predicted by the Marcus equations.[18,68] These barriers are also given in Table I and as expected are similar to those of Grimsrud et al.[38] The $E^{\ddagger}$ obtained in this manner were found[38] in qualitative agreement with the kinetic results (Table II and Figure 7). However, the magnitude of $\Delta E_0^{\ddagger}$, which is the parameter that controls the magnitude of k, does not depend directly on $E^{\ddagger}$ but is given by $\Delta E_0^{\ddagger} = E^{\ddagger} - D(A^-\text{–}B)$, where $D(A^-\text{–}B)$ is the bond energy of the stable $A^-\cdot B$ complex at the bottom of the first well (see Figure 8). The qualitative agreement was obtained with an estimated value of $D(SF_6^-\text{–}B)$.[38] Actual measurements of $D(SF_6^-\text{–}B)$ and $D(SF_6\text{–}B^-)$ were performed[72] by measuring the temperature dependence of equilibria $SF_6^- + B = SF_6^-\cdot B$ and $B^- + SF_6 = B^-\cdot SF_6$ (see section VI). The results were surprising.[72] It was found that SF_6^- bonds to B quite strongly, but negative ions B^- bond to SF_6 very weakly. The weak bonding of negative ions to SF_6 was attributed to the unfavorable dodecapole moment of SF_6, i.e., to the negative charge outer "envelope" in SF_6 caused by the large electronegativity of the F atoms.[72] The strong bonding in $SF_6^-\cdot B$ increases $-\Delta E_0^{\ddagger}$ while the weak bonding in $SF_6\cdot B^-$ decreases it again. Furthermore, the structures of $SF_6^-\cdot B$ and $SF_6\cdot B^-$ are probably also quite different due to the different type of bonding in $SF_6^-\cdot B$ and $SF_6\cdot B^-$ (see section VI). This structural difference would also increase the barrier in Figure 8 and be an additional factor reducing the rate of reaction 12.

It was concluded[72] that reaction 12 and probably also the reactions involving the perfluorocycloalkanes are slow because the geometries of the neutral perfluoro compound and its negative ion are quite different. Additional factors slowing down the rate are the low binding energies of the perfluoro negative ions to molecules B and the different structures of the complexes $A^-\cdot B$ and $A\cdot B^-$.

Differences of bond energies and structures of the complexes $A^-\cdot B$ and $A\cdot B^-$ are not considered as possible factors affecting electron transfer in solution.[18] This is probably justified since solvation of the ions reduces the bonding in $A^-\cdot B$ and $A\cdot B^-$ to almost zero.

IV. Electron Affinities: Structures and Stabilities of Radical Anions

A. Substituted Aromatic Compounds

The electron affinities of substituted aromatic compounds are given in Table II. The large majority of the data are first determinations. Furthermore, the data represent the first comprehensive compilation covering a wide variety of compounds. This justifies a brief examination of the parameters determining the magnitude of the electron affinities for the classes of compounds.

Benzene is the progenitor of the other aromatic compounds. The added electron enters the lowest unoccupied orbital (LUMO), which in the negative ion becomes the singly occupied molecular orbital (SOMO). The LUMO is a π^* type orbital, and the π orbital diagram is shown in Chart I. The lower the energy of the LUMO the higher will be the electron affinity. In benzene, the LUMO energy is still high and a stable negative ion is not formed in the gas phase.

CHART I

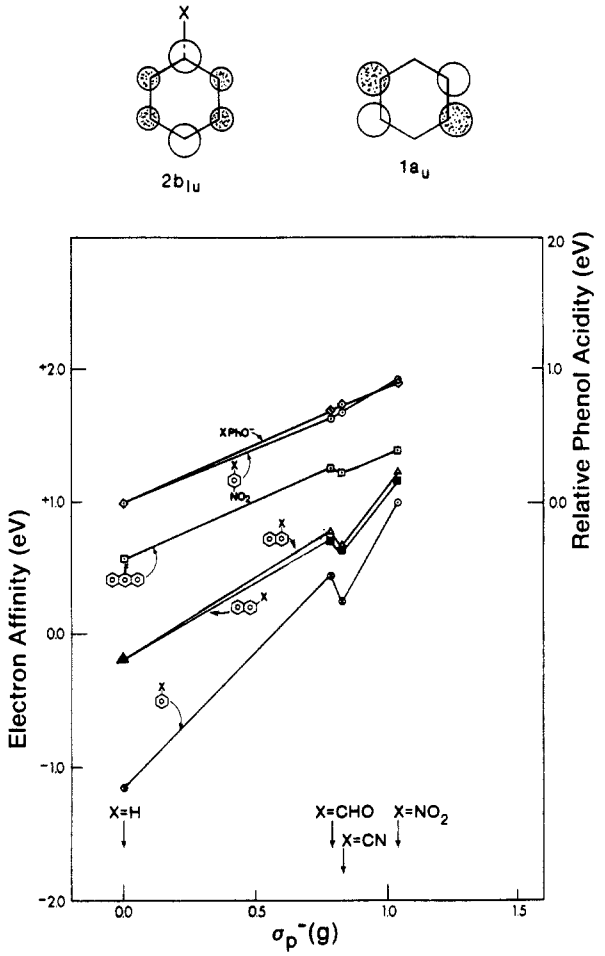

Figure 10. Electron affinities of substituted benzenes, naphthalenes, anthracenes, and nitrobenzenes. The negative electron affinities for benzene and naphthalene are from Jordan.[73] The corresponding negative ions are unstable. A decreasing substituent effect (decreasing slope ρ) is observed as the charge delocalization of the first member negative ion increases. σ_p-(g) are Hammet substituent constants from Taft.[75] From Chowdhury.[44]

The LUMO energy can be lowered either by expansion of the π conjugation or by introduction of electron-withdrawing substituents. This was illustrated by Chowdhury et al.[44] on the basis of the EA data, as shown in Figure 10. For the unsubstituted benzene, naphthalene, and anthracene the EA is seen to increase. A positive EA, i.e., a stable negative ion, is observed only for anthracene. The negative electron affinities[73] for benzene and naphthalene given in Figure 10 correspond to the energy required to put an electron into the LUMO of the molecules. The resulting negative-ion states formed are short-lived (10^{-12}–10^{-15} s). Negative electron affinities are successfully measured by electron transmission spectroscopy (ETS).[73]

Polyaromatic hydrocarbons with more rings than anthracene have progressively lower LUMO's and thus are expected to have progressively higher positive electron affinities.[74]

Electron-withdrawing substituents like CHO, CN, and NO_2 lead to large increases of electron affinity (see Figure 10). The effect of a given substituent is seen to decrease from benzene to anthracene, i.e., in the order of increasing negative charge delocalization in the unsubstituted anion. The lowest slope, i.e., the lowest effect of the substituent, is observed for substituted

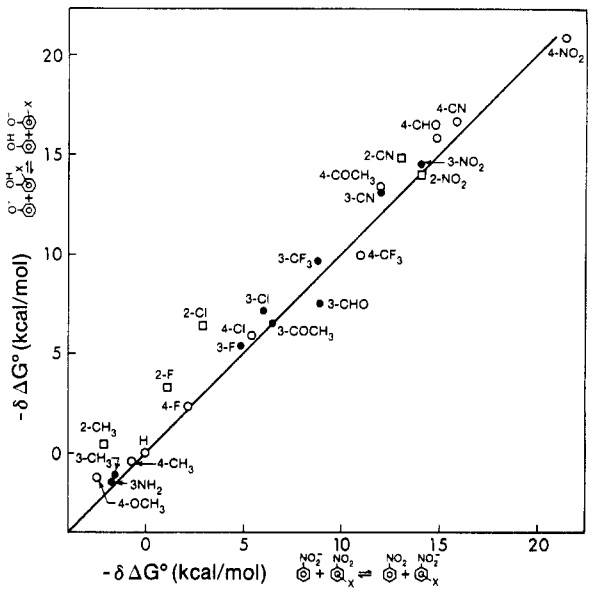

Figure 11. Plot of electron affinities of substituted nitrobenzenes vs. gas-phase acidities of substituted phenols (see eq 13). A linear relationship with unit slope is observed. From Fukuda[33] and Grimsrud.[37]

nitrobenzenes (see Figure 10). In these systems charge delocalization in the unsubstituted compound (nitrobenzene$^-$) is due to delocalization onto the NO_2 group.[44]

More extensive EA data are available for substituted nitrobenzenes from ETE determinations in both McIver's and Kebarle's laboratory (see Table II). A plot of the substituent effects is shown in Figure 11. The substituent constant magnitudes, σ_p^- (Figure 10), were chosen by Taft[75] on the basis of the gas-phase acidities of substituted phenols. This choice means that σ_p^- and the proton-transfer free energies, $\Delta G_{13}°$, are linearly related. The close correlation between substituent

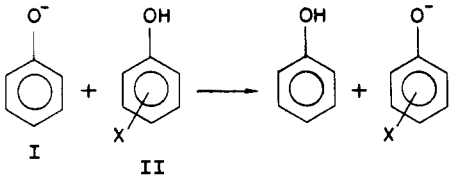

(13)

effects on the acidities of phenols and on the electron affinities of nitrobenzenes is remarkable, particularly when one considers that the electron in the phenoxide anions is in a π type orbital while that in the nitrobenzene radical anion is in a π^* orbital. From a practical standpoint, it is evident that σ_p^- values can be used with some confidence to predict electron affinities of substituted nitrobenzenes that have not been measured.

The reversals of the CHO and CN substituent effects on the electron affinities of the less charge delocalized substituted benzenes, naphthalenes, and anthracenes (see Figure 10) have been attributed[44] to the greater increase of the π electron withdrawing effect relative to the field effect, with decreasing charge delocalization in the unsubstituted ion. Thus the strongly π withdrawing CHO substituent becomes relatively more effective than the strong field effect stabilizing CN in the weakly delocalized systems, i.e., toward the bottom of Figure 10.

Informative theoretical (STO-3G) molecular orbital calculations on benzene and substituted benzene radical anions have been reported by Radom.[76] While the en-

ergies of the two π^* LUMOs in benzene are the same, a splitting of energy occurs after the extra electron is added (Jahn–Teller effect). In benzenes substituted with an electron-withdrawing substituent X, the $2b_{1u}$ state (Chart I) leads to lower energy, while electron-donating substituents favor the $1a_u$ state. The presence of the electron leads to (small) changes of C–C bond lengths in the ring. The distance shortens between the C atoms for which the psi density is in phase, as is the case for the two pairs of neighboring shaded atoms in the $2b_{1u}$ state (see Chart I).

Energy changes with substitution for benzene negative ions calculated by Radom were found in approximate agreement with experimental electron affinity changes.[76]

Data on the stabilities of substituted aromatic radical anions in solution are available from polarographic half-wave potentials. These results are compared with the gas-phase electron affinities in section VI, which deals with the solvation energies of radical anions.

B. Substituted Benzo-, Naphtho-, and Anthraquinones

The quinones are an extremely important group of compounds in both biochemistry and organic chemistry. In biochemistry, quinones, attached to proteins, are the prosthetic group involved in electron and hydrogen transfers.[13,76–78] The one- or two-electron reduction of quinone (quinone–hydroquinone) is reversible and represents an important example of organic electrochemistry.

Diels–Alder reactions involving cycloadditions of dienes to quinones are valuable routes for the synthesis of many natural products. Because the majority of cycloadditions and additions to quinones involve electron-rich species (nucleophiles), the low energy of the LUMO of quinones is an important factor in these reactions.[81]

The LUMO's of quinone and naphthoquinone, which accommodate the extra electron, are shown in Chart II. Both Hückel MO[82] and STO-3G calculations[81] predict a lower LUMO energy for benzoquinone relative to naphthoquinone. Thus for the quinones, one expects a decrease of electron affinities from benzoquinone to naphthoquinone to anthroquinone. This agrees with the experimentally measured electron affinities (see Table II). The decrease of electron affinities in the above order is opposite to that observed for benzene, naphthalene, and anthracene (see preceding section).

p-Quinodimethane (III) has substantial delocalization energy (1.924β), which is similar to that of benzene (2β).

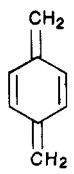

III

Probably it still has, like benzene, a negative electron affinity.[83] Thus, the substantial electron affinity of quinone, EA = 42.4 kcal/mol, is due to the high electronegativity of the two oxygen atoms, which leads to a substantial lowering of the LUMO energy.

The electron affinities of some 21 substituted benzo-, naphtho-, and anthroquinones measured by ETE[37,46a] are given in Table II. Substantial increases of EA are observed for multiple substitution with electron-withdrawing groups. Thus tetrachlorobenzoquinone has an electron affinity that is higher by 20 kcal/mol than that of benzoquinone.

Methyl substitution on the sp^2 hybridized carbons of the quinones leads to a lowering of the electron affinity (see Table II). A similar effect was observed for methyl-substituted nitrobenzenes. Methyl on sp^2 carbon is known to be destabilizing for negatively charged species. This effect is responsible for the higher gas-phase acidity of acetylene relative to methylacetylene and formic acid relative to acetic acid.[84,85]

Fukuda and McIver[33,34] have reported the relative electron affinities of 21 substituted quinones. These results were based on $\Delta G_1°$ scales (see section II). In order to achieve a comparison the Fukuda scale was calibrated by the present authors to $-\Delta G_a(SO_2) = 26.1$ kcal/mol. Electron affinities of quinones measured in both laboratories are shown in Figure 12. The values are seen to be in very good agreement except for perfluorobenzoquinone for which the PHPMS result is some 5 kcal/mol higher. The total Fukuda and McIver $\Delta G_a°$(B) are given in Table II.

Cooper et al.[86,87] have determined some quinone electron affinities with a Cs atom beam collisional ionization technique. These values are compared with the ETE values in parentheses: benzoquinone 1.89 (1.91) eV, tetrafluoroquinone 2.9 (2.7) eV, and tetrachloroquinone 2.78 (2.76) eV (Table II). The agreement is very good except for the perfluoro compound. Cooper's

CHART II. LUMO's of Benzo- and Naphthoquinone[a] [81]

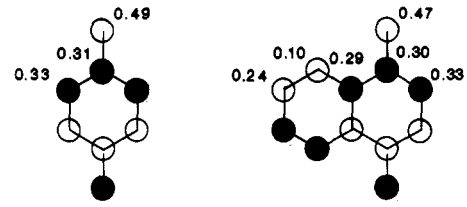

[a] The numbers are LUMO coefficients obtained from STO-3G calculations.

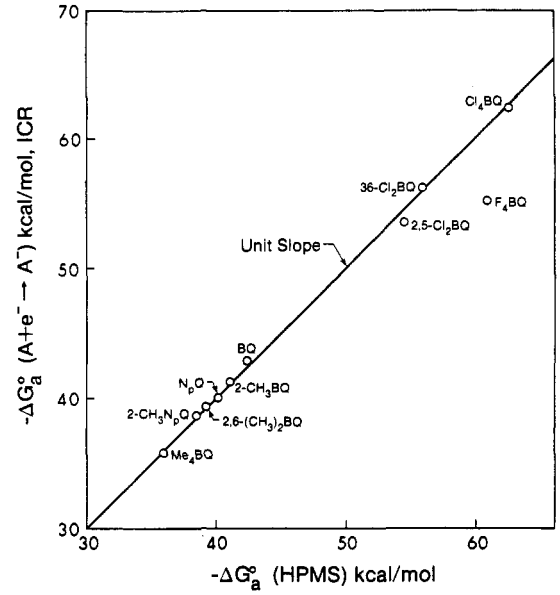

Figure 12. Comparison of ETE results leading to electron affinities of substituted quinones determined by ICR (McIver[33,34]) and PHPMS.[37,46a]

TABLE II. Electron Affinities

molecule[a]	$-\Delta G_a°$,[b] kcal/mol PHPMS	ICR	$-\Delta H_a° \approx$ EA; ETE[c] ±0.1, eV	EA,[d] eV
		Triatomic		
NO_2 (nitrogen dioxide)	52.6	–	2.30 (41)	2.28 ± 0.1 (ECT, 50); 2.36 ± 0.1 (LPD, 98); ≥2.5 ± 0.1 (CI, 99); 2.28 ± 0.025 (LPD, 100); ≥2.32, ≤2.5 (KB, 101); 2.1 (ECT, 105); 2.5 (CI, 103)
SO_2 (sulfur dioxide)	(26.1)	(26.1)	(1.10)	≤1.0 ± 0.1 (PD, 104); 1.05 (ECT, 53); 0.99 ± 0.1 (ECT, 50); 1.14 ± 0.15 (CI, 53); 1.097 ± 0.036 (PES, 49)
CS_2 (carbon disulfide)	12.7	–	0.51 (41)	0.50 ± 0.2 (ECT, 50); 1.0 ± 0.2 (CI, 110); 0.62 ± 0.2 (CI, 111)
		Polyatomic		
CH_3NO_2 (nitromethane)	12.1	–	0.48 (41)	0.44 ± 0.1 (CI, 107)
$C_4H_2N_2$ (*trans*-1,2-dicyanoethylene)	28.4	–	1.24 (43)	
$C_4H_6O_2$ (2,3-butanedione)	16.9	–	0.69 (41)	0.63 ± 0.05 (ECD, 108)
C_6N_4 (tetracyanoethylene)	73.0	–	3.17 (43)	2.3 ± 0.3 (PD, 114); 2.9 (M, 115); 2.9 (CTS, 116)
		Substituted Benzenes		
2,3-$C_6H_3Cl_2NO_2$ (2,3-dichloronitrobenzene)	–	29.1		
3,4-$C_6H_3Cl_2NO_2$ (3,4-dichloronitrobenzene)	–	32.6		
2-$C_6H_4BrNO_2$ (*o*-bromonitrobenzene)	26.3	–	1.17 (41)	
2-$C_6H_4BrNO_2$ (*o*-bromonitrobenzene)	26.2	–	1.16 (41)	
3-$C_6H_4BrNO_2$ (*m*-bromonitrobenzene)	29.5	–	1.32 (41)	
4-$C_6H_4BrNO_2$ (*p*-bromonitrobenzene)	29.0	–	1.29 (41)	
2-$C_6H_4ClNO_2$ (*o*-chloronitrobenzene)	25.7	25.1	1.14 (41)	
3-$C_6H_4ClNO_2$ (*m*-chloronitrobenzene)	28.8	28.4	1.28 (41)	
4-$C_6H_4ClNO_2$ (*p*-chloronitrobenzene)	28.2	27.7	1.26 (41)	
2-$C_6H_4FNO_2$ (*o*-fluoronitrobenzene)	24.2	24.9	1.07 (41)	
3-$C_6H_4FNO_2$ (*m*-fluoronitrobenzene)	27.7	27.2	1.23 (41)	
4-$C_6H_4FNO_2$ (*p*-fluoronitrobenzene)	25.0	24.7	1.12 (41)	
2-$C_6H_4N_2O_4$ (*o*-dinitrobenzene)	36.9	–	1.65 (41)	1.66 ($E_{1/2}$, 116); 1.07 (CTS, 116)
3-$C_6H_4N_2O_4$ (*m*-dinitrobenzene)	36.9	37.0	1.65 (41)	1.58 ($E_{1/2}$, 116); 1.26 (CTS, 116)
4-$C_6H_4N_2O_4$ (*p*-dinitrobenzene)	44.3	44.4	2.00 (41)	
$C_6H_5NO_2$ (nitrobenzene)	22.8	23.1	1.01 (41)	>0.8 ± 0.2 (ECD, 108a); ≥0.7 ± 0.2 (ECT, 50)
3-$C_6H_6N_2O_2$ (*m*-nitroaniline)	21.0	–	0.95 (43)	
2,6-$C_7H_3Cl_2N$ (2,6-dichlorobenzonitrile)	16.7	–	0.72 (43)	
3,5-$C_7H_3N_3O_4$ (3,5-dinitrobenzonitrile)	48.5	–	2.16 (41)	
2-$C_7F_3NO_2$ (*o*-α,α,α-trifluoromethylnitrobenzene)	29.9	–	1.33 (47)	
3-$C_7H_4F_3NO_2$ (*m*-α,α,α-trifluoromethylnitrobenzene)	31.6	31.5	1.41 (47)	
4-$C_7H_4F_3NO_2$ (*p*-α,α,α-trifluoromethylnitrobenzene)	33.8	–	1.47 (47)	
2-$C_7H_4N_2O_2$ (*o*-nitrobenzonitrile)	35.8	–	1.61 (41)	
3-$C_7H_4N_2O_2$ (*m*-nitrobenzonitrile)	34.8	35.2	1.56 (41)	
4-$C_7H_4N_2O_2$ (*p*-nitrobenzonitrile)	38.7	–	1.72 (41)	
2-$C_7H_5NO_3$ (*o*-nitrobenzaldehyde)	34.6	–	1.51 (47)	
3-$C_7H_5NO_3$ (*m*-nitrobenzaldehyde)	31.7	–	1.41 (47)	
4-$C_7H_5NO_3$ (*p*-nitrobenzaldehyde)	37.7	–	1.67 (47)	
2,4-$C_7H_6FNO_2$ (2-methyl-4-fluoronitrobenzene)	22.7			
2,3-$C_7H_6N_2O_4$ (2-methyl-3-nitrobenzene)		38.8		
2-$C_7H_7NO_2$ (*o*-nitrotoluene)	20.7	21.4	0.92 (41)	
3-$C_7H_7NO_2$ (*m*-nitrotoluene)	22.1	22.1	0.99 (41)	
4-$C_7H_7NO_2$ (*p*-nitrotoluene)	21.2	21.7	0.95 (41)	
3-$C_7H_7NO_3$ (*m*-methoxynitrobenzene)	23.4	–	1.04 (41)	
4-$C_7H_7NO_3$ (*m*-methoxynitrobenzene)	20.3	–	0.91 (41)	
3,5-$C_8H_3F_6NO_2$ (3,5-bis(α,α,α-trifluoromethyl)nitrobenzene)	40.2	–	1.79 (41)	
2-$C_8H_4F_3N$ (*o*-α,α,α-trifluoromethylbenzonitrile)	15.8	–	0.70 (43)	
3-$C_8H_4F_3N$ (*m*-α,α,α-trifluoromethylbenzonitrile)	15.5	–	0.67 (43)	
4-$C_8H_4N_2$ (*p*-α,α,α-trifluoromethylbenzonitrile)	18.6	–	0.76 (43)	
2-$C_8H_4N_2$ (*o*-cyanobenzonitrile)	22.3	–	0.95 (43)	1.11 ± 0.13 (M, 115)
3-$C_8H_4N_2$ (*m*-cyanobenzonitrile)	21.0	–	0.91 (43)	
4-$C_8H_4N_2$ (*p*-cyanobenzonitrile)	25.8	–	1.10 (43)	
3-C_8H_5NO (*m*-cyanobenzaldehyde)	23.2	–	1.00 (43)	
4-C_8H_5NO (*p*-cyanobenzaldehyde)	28.1	–	1.22 (43)	
2-$C_8H_7NO_3$ (*o*-nitroacetophenone)	30.9	–	1.38 (47)	
3-$C_8H_7NO_3$ (*m*-nitroacetophenone)	29.3	–	1.31 (47)	
4-$C_8H_7NO_3$ (*p*-nitroacetophenone)	34.8	–	1.55 (47)	
2-$C_8H_8O_2$ (*o*-hydroxyacetophenone)		20.7		
2,3-$C_8H_9NO_2$ (2,3-dimethylnitrobenzene)	19.4	20.7	0.86 (41)	
3,4-$C_8H_9NO_2$ (3,4-dimethylnitrobenzene)		20.9		
2,4-$C_8H_9NO_2$ (2,4-dimethylnitrobenzene)		20.1		
2,6-$C_8H_9NO_2$ (2,6-dimethylnitrobenzene)	–	18.3		
3-$C_8H_{10}N_2O_2$ (*N,N*-dimethyl-3-nitroaniline)	–	22.0		
3,5-$C_9H_3F_6N$ (3,5-bis(α,α,α-trifluoromethyl)benzonitrile)	26.3	–	1.14 (43)	
4-C_9H_7NO (*p*-cyanoacetophenone)	25.0		1.13 (43)	

TABLE II (Continued)

molecule[a]	$-\Delta G_a°$,[b] kcal/mol PHPMS	ICR	$-\Delta H_a° \approx$ EA; ETE[c] ±0.1, eV	EA,[d] eV
2,4,6-$C_9H_{11}NO_2$ (2,4,6-trimethylnitrobenzene)	16.1	17.5	0.70 (41)	
3-$C_{12}H_9NO_2$ (*o*-nitrobiphenyl)	23.8	–	1.07 (47)	
3-$C_{12}H_9NO_2$ (*m*-nitrobiphenyl)	25.1	–	1.13 (47)	
4-$C_{12}H_9NO_2$ (*p*-nitrobiphenyl)	26.9	–	1.20 (47)	
$C_{13}H_8F_2O$ (4,4′-difluorobenzophenone)	–	19.1		
$C_{13}H_9ClO$ (4-chlorobenzophenone)	–	20.4		
$C_{13}H_9FO$ (4-fluorobenzophenone)	15.8	17.9	0.64 (41)	
$C_{13}H_{10}O$ (benzophenone)	15.3	16.7	0.62 (41)	0.64 ± 0.1 (ECD, 108)
Perfluoro Compounds				
C_6F_6 (hexafluorobenzene)	14.8	–	0.52 (42)	>1.8 ± 0.3 (ECT, 50)
C_7F_8 (α,α,α-trifluoromethylpentafluorobenzene)	21.6	–	0.94 (42)	>1.7 + 0.3 (ECT, 50)
C_7H_5N (pentafluorobenzonitrile)	27.0	–	1.1 (42)	
$C_8H_3F_5O$ (pentafluoroacetophenone)	21.7	–	0.94 (2)	
1,4-$C_8F_4N_2$ (1,4-dicyanotetrafluorobenzene)	43.5		1.89 (42)	
$C_{12}F_{10}$ (perfluorobiphenyl)	20.9	–	0.91 (42)	
$C_{13}F_{10}O$ (decafluorobenzophenone)	37.1	–	1.61 (42)	
SF_6	29.3	–	1.05 (38)	0.75 ± 0.1 (CI, 103); >0.6 ± 0.1 (ECT, 50); 0.54 ± 0.1 (CI, 110); 0.46 ± 0.2 (CI, 107); 1.0 ± 0.2 (KB, 65)
C_7F_{14} (perfluoromethylcyclohexane)	26.0	–	1.06 (38)	
Azulene, Naphthalenes, and Anthracenes				
$C_{10}H_8$ (azulene)	18.0	–	0.69 (39, 41)	0.66 (ECD, 108b) 0.65 (ECD, 108c)
$C_{10}H_7NO_2$ (1-NO_2 naphthalene)	27.9	–	1.23 (45)	
$C_{10}H_7NO_2$ (2-NO_2 naphthalene)	26.8	–	1.18 (45)	
$C_{10}H_6N_2O_4$ (1,3-dinitronaphthalene)	39.7	–	1.78 (45)	
$C_{10}H_6N_2O_4$ (1,5-dinitronaphthalene)	39.3	–	1.77 (45)	
$C_{11}H_7N$ (1-naphthonitrile)	15.6	–	0.68 (45)	
$C_{11}H_7N$ (2-naphthonitrile)	14.9	–	0.65 (45)	
$C_{11}H_8O$ (1-naphthaldehyde)	17.8	–	0.70 (45)	0.68 ± 0.03 (ECD, 11b)
$C_{11}H_8O$ (2-naphthaldehyde)	16.4	–	0.65 (45)	0.62 ± 0.03 (ECD, 11b)
$C_{11}H_9NO_2$ (2-methyl-1-nitronaphthalene)	23.0	–	1.03 (45)	
$C_{11}N_9NO_3$ (4-methoxy-1-nitronaphthalene)	24.5	–	1.10 (45)	
$C_{14}H_{10}$ (anthracene)	13.2	–	0.60 (45)	0.556 (ECD, 108b)
$C_{14}H_9Cl$ (1-chloroanthracene)	18.0	–	0.78 (45)	
$C_{14}H_9Cl$ (2-chloroanthracene)	17.4	–	0.75 (45)	
$C_{14}H_9Cl$ (9-chloroanthracene)	18.7	–	0.86 (45)	
$C_{14}H_9NO_2$ (9-nitroanthracene)	31.8	–	1.43 (45)	
$C_{15}H_9N$ (9-cyanoanthracene)	28.2	–	1.27 (45)	
$C_{15}H_{10}O$ (9-anthraldehyde)	29.0	–	1.31 (45)	
$C_{16}H_{12}O$ (9-acetylanthracene)	22.3	–	0.97 (45)	
Benzo-, Naphtho-, and Anthraquiones				
$C_6Cl_4O_2$ (tetrachloro-*p*BQ)	62.6	62.3	2.78 (41, 46a)	2.76 ± 0.2 (CI, 87)
$C_6F_4O_2$ (tetrafluoro-*p*BQ)	60.9	55.2	2.70 (41, 46a)	2.92 ± 0.2 (CI, 87)
$C_6HCl_3O_2$ (trichloro-*p*BQ)	–	5.90		
$C_6H_2Cl_2O_2$ (2,6-dichloro-*p*BQ)	55.8	56.1	2.48 (41)	
$C_6H_2Cl_2O_2$ (2,5-dichloro-*p*BQ)	54.7	53.5	2.43 (41)	
$C_6H_4O_2$ (pBQ)	42.4	43.0	1.91 (41, 46a)	1.89 ± 0.2 (CI, 86)
$C_7H_3Cl_3O_2$ (methyltrichloro-*p*BQ)	–	57.5		
$C_7H_5ClO_2$ (2-chloro-5-methyl-*p*BQ)	–	47.5		
$C_7H_6O_2$ (2-methyl-*p*BQ)	41.1	41.3	1.85 (41)	
$C_8H_6Cl_2O_2$ (2,5-dichloro-3,6-dimethyl-*p*BQ)	–	50.2		
$C_8H_7ClO_2$ (2-chloro-3,6-dimethyl-*p*BQ)	–	45.3		
$C_8H_8O_2$ (2,6-dimethyl-*p*BQ)	39.3	39.4	1.78 (46a)	
$C_8H_8O_2$ (2,5-dimethyl-*p*BQ)	39.2	–	1.77 (46a)	
$C_8H_8O_4$ (2,6-dimethoxy-*p*BQ)	38.9	–	1.73 (46a)	
$C_9H_9ClO_2$ (chlorotrimethyl-*p*BQ)	–	43.8		
$C_9H_{10}O_2$ (trimethyl-*p*BQ)	–	37.7		
$C_9H_{10}O_1$ (2,3-dimethoxy-5-methyl-*p*BQ)	40.8	–	1.86 (46a)	
$C_{10}H_4Cl_2O_2$ (2,3-dichloro-1,4-NpQ)	49.2	–	2.19 (41)	
$C_{10}H_6O_2$ (1,4-NpQ)	40.2	40.1	1.81 (4)	>0.8 ± 0.2 (ECD, 108a)
$C_{10}H_9BrCl_2O_2$ (2,6-dichlorobromo-*tert*-butyl-*p*BQ	–	56.6	–	
$C_{10}H_{10}Cl_2O_2$ (2,3-dichloro-*tert*-butyl-*p*BQ)	–	52.6		
$C_{10}H_{11}ClO_2$ (2-chloro-5-*tert*-butyl-*p*BQ)	–	48.3		
$C_{10}H_{12}O_2$ (1-isopropyl-5-methyl-*p*BQ)	39.9	–	1.79 (46a)	
$C_{10}H_{12}O_2$ (*tert*-butyl-*p*BQ)		42.4		
$C_{10}H_{12}O_2$ (tetramethyl-*p*BQ)	36.0	35.9	1.59 (46a)	
$C_{11}H_8O_2$ (2-methyl-1,4-NpQ)	38.5	38.7	1.74 (46a)	
$C_{12}H_8O_2$ (2-phenyl-*p*BQ)	45.1	–	2.04 (46a)	
$C_{14}H_7ClO_2$ (1-chloro-9,10-AnQ)	38.3	–	1.71 (46a)	
$C_{14}H_8O_2$ (9,10-AnQ)	35.4	–	1.59 (46a)	
$C_{14}H_{20}O_2$ (2,6-di-*t*-Bu-pBQ)	41.4	–	1.88 (46a)	

TABLE II (Continued)

molecule[a]	$-\Delta G_a°$,[b] kcal/mol PHPMS	ICR	$-\Delta H_a° \approx$ EA; ETE[c] ±0.1, eV	EA,[d] eV
$C_{16}H_{12}O_2$ (2-Et-9,10-AnQ)	34.7	-	1.56 (46a)	
$C_{18}H_{16}O_2$ (2-*t*-Bu-9,10-AnQ)	34.7	-	1.56 (46a)	
Unsaturated (Cyclic) Diketonic Compounds				
$C_4H_2O_3$ (maleic anhydride)	33.1	32.7	1.44 (41)	>1.4 (CI, 99)
$C_8H_4O_3$ (phthalic anhydride)	27.8	27.4	1.21 (41)	

[a] Abbreviations used: *p*BQ, 1,4-benzoquinone; NpQ, 1,4-naphthoquinone; AnQ, antraquinone. [b] $\Delta G_a°$ is the free energy change for stationary electron attachment. PHPMS, results are from the present laboratory[37-39,41-47] at 423 K; ICR, results are from Fukuda and McIver at 353 K. In order to obtain $\Delta G_a°$, Fukuda's results are anchored to $\Delta G_a°(SO_2) = -26.1$ kcal/mol. [c] The results presented in this column are from PHPMS determinations. van't Hoff plots are made involving some 40 molecules; for the rest of the molecules $\Delta S_a°$ is estimated (see appropriate reference given in parentheses). The estimated error for the EA values is ±0.1 eV, except ±0.2 eV for C_6N_4, tetracyanoethylene. [d] The electron affinity values given in this column are gas-phase values available in the literature. Some condensed-phase electron affinity values are also given. Reference number and technique are given in parentheses, and the notation indicates the name of the technique: ECT, endothermic charge-transfer method; LPD laser photodetachment technique; CI, collisional ionization technique; ECD, electron capture detector technique; M, magnetron method; CTS, charge-transfer spectroscopic method in solution; $E_{1/2}$, half-wave reduction potential method in solution; KB, kinetic bracketing technique.

high value for tetrafluoroquinone is probably incorrect since one expects chloro substitution to lead to higher EA than fluoro substitution (see chloro- vs. fluoro-substituted nitrobenzenes (Table II) and also results of Fukuda and McIver (Table II) for the quinones which give a higher $-\Delta G_a°$ for the tetrachloroquinone).

Additional discussion of substituent effects on the EA's of quinones can be found in Heinis et al.[46a]

The electron affinities of maleic anhydride IV and phthalic anhydride V, determined by ETE by Chowdhury et al.,[41] are given in Table II. These compounds,

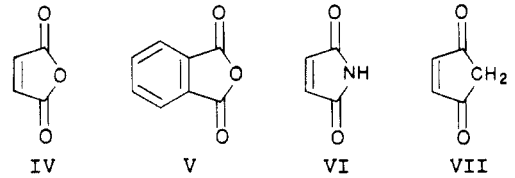

IV V VI VII

whose structures resemble those of the corresponding quinones except that there is only one double bond rather than two in the quinoid structure, have lower electron affinities than the corresponding quinones. The EA of the NH and the CH_2 bridged compounds VI and VII were also determined.[88] It was found,[88] as could be expected, that the EA decreases as the electronegativity of the bridging atom decreases, i.e., in the order O, NH, CH_2.

Extensive data on the stabilities of quinone radical anions in solution are available from polarographic half-wave potentials. These results are compared with the gas-phase EA in section V, which deals with the solvation energies of radical anions.

C. Hexafluorobenzene, Substituted Perfluorobenzenes, SF_6, and Perfluorocycloalkanes

The high electronegativity of F leads to a lowering of the LUMO energies and thus an increase of electron affinity with fluoro substitution and particularly perfluorination. However, the energy lowering occurs to a much lesser extent for π^* relative to σ^* LUMO's. Fluorine is strongly "electron withdrawing" by the field effect but is (weakly) electron pair donating (π donation). Therefore σ^* orbitals are strongly stabilized by the field effect, while the diffuse π^* orbitals are less strongly stabilized by the field effect and destabilized by the π donation.[89]

Benzene has a negative electron affinity, EA = −1.15 eV,[73,90] as does fluorobenzene, EA = −0.89 eV,[90] which means that single fluorine substitution leads to an EA increase of 0.26 eV. Radom et al.[26] have obtained a similar change on the basis of STO-3G calculations. This relatively small increase is in line with the expected weak stabilization of a π^* orbital by fluorine. In view of the above numbers, positive electron affinities for fluorobenzenes can be expected only after multiple fluorine substitution. An early measurement[91] of EA-(C_6F_6) ≥ 1.8 eV by the endothermic charge-transfer technique (ECT) is much higher than the recent ETE value[42] of 0.52 eV. The ETE determinations (Table II) include a whole group of substituted perfluorobenzenes. These values were found[42] to be consistent with expected substituent effects. For example, perfluorotoluene has an EA of 0.94 eV,[42] considerably higher than that for C_6F_6 of 0.52 eV, as expected since the CF_3 group in the toluene should have a much stronger electron-withdrawing effect than the F atom that it replaces. On the other hand, ECT gave EA($C_6F_5CF_3$) ≥ 1.7 eV which is *lower* than the ECT value for C_6F_6 of 1.8 eV. The ECT C_6F_6 value appears also much too high when compared to the 0.26-eV increase from C_6H_6 to C_6H_5F discussed above. For six F substitutions one would expect an increase of 6 × 0.26 eV = 1.6 eV, or an EA-(C_6F_6) ≈ 0.41 eV. This crude estimate leads to a value close to the ETE result of 0.52 eV.

Some structural information on the geometry of $C_6F_6^-$ is available on the basis of electron spin resonance coupling constants measured in the condensed phase.[92,93] The resulting geometry depends on the theoretical treatment and greatly differing geometries: carbon skeleton distorted to a cyclohexane like chair[92,93] and undistorted carbon skeleton but out of plane C–F bonds[94] have been proposed.

The error in the EA measurement of C_6F_6 by the ECT method[91] is probably due to the change of geometry between C_6F_6 and $C_6F_6^-$. Difficulties in EA determinations of perfluoro compounds are not restricted to C_6F_6 but are encountered also for SF_6 and the perfluorocyclohexanes. In these cases also, changes of geometry between A and A^- could be at least partially responsible for discrepancies between available determinations.

Some 19 determinations of the electron affinity of SF_6 have been reported in the literature. For a summary see Table IV in Streit.[65] The values range from 0.53 to

1.5 eV. The five most recent determinations are given in Table II. The ETE value by Grimsrud et al.,[38] EA(SF_6) = 1.05 eV, is in good agreement with the recent determination of Streit[65] based on the kinetic bracketing technique. The study of the kinetics of electron transfer involving SF_6 by Grimsrud et al.[38] is summarized in Table IB. Grimsrud et al. found that electron transfer involving SF_6 was very slow. A large change of geometry between SF_6 and SF_6^- was assumed to be the primary reason for the slow rates. The slowness of the rates made the ETE measurements more difficult,[38] although conditions were found under which the ETE could be measured.

An electron affinity EA(SF_6) $\approx$ 1 eV was obtained by Hay[70] from SCF-MO calculations of the energies of SF_6 and SF_6^-. This value is in good agreement with the ETE[38] and the bracketing[65] result. However, the agreement may be fortuitous. It would seem that reliable theoretical results would require much more extensive calculations. The LUMO of SF_6 is a σ^* type orbital with s, p, and d atom orbital contributions.[70]

Hay,[70] assuming SF_6^- retains the regular octahedral symmetry of SF_6, found that the S–F bond lengthens considerably in SF_6^- (see Figure 9). Brauman[69] has provided some semiempirical evidence that SF_6^- may resemble SF_5^-·F. Lifshitz[91] has examined electron autodetachment lifetimes for SF_6^- on the basis of RRKM theory. Assuming the model of Brauman,[69] Lifshitz determined an EA(SF_6) of $\approx$1 eV.[91]

The electron affinity of 1.06 eV for perfluoromethylcyclohexane was determined by ETE measurements[38] (Table II). The value is quite high if one considers that a fairly localized σ^* type LUMO must be involved. Perfluorocyclohexane also forms a stable negative ion.[38] Both perfluoro negative ions, $C_6F_{12}^-$ and $C_6F_{11}CF_3^-$, were found to be extremely unreactive in electron transfer. This was attributed to large geometry changes between the neutrals and the negative ions.[38,72]

Molecules like SF_6, C_6F_{12}, and $C_6F_{11}CF_3$, which have relatively high electron affinities, high thermal electron capture cross sections, and negative ions that are very unreactive toward electron transfer, are good electron scavengers and dielectrics,[95,96] preventing electrical breakdown since they capture electrons efficiently and retain them.

D. Triatomic Molecules, Tetracyanoethylene, and Miscellaneous Compounds

A number of electron affinity determinations are available for NO_2[98-103] and SO_2[49,104-107] (see Table II). The measurement of SO_2 by Hall et al.[49] led to a photoelectron spectrum with distinct vibrational structure that could be successfully analyzed. The EA(SO_2) = 1.097 eV should be a very reliable value and was used (see section II) as the anchor compound in the ETE measurements from this laboratory. Hirao[109] published recently a theoretical calculation including electron correlation which provides EA(SO_2) = 1.027 eV in good agreement with the experimental result.[49]

Photodetachment results[98,100] for NO_2 gave threshold curves without distinct vibrational structure. However, available vibrational spacing information for NO_2^- observed in solution could be used to achieve a fairly reliable fit of the curves and an identification of the adiabatic electron affinity. The relatively good agreement of the ETE result for NO_2 with the photodetachment data (see Table II) lends confidence to the ETE measurements. NO_2 is not very suitable as a secondary standard in ETE measurements because of the readiness with which NO_2^- engages in ion–molecule reactions with other compounds.[40] The ETE result EA(CS_2) = 0.51 eV is seen to be in agreement with two of the three literature values.[106,110,111] Although the literature data are absolute determinations, the reliability of the ETE result is probably superior. The same is true for the data for nitromethane and 2,3-butanedione shown in Table II.

Tetracyanoethylene is a compound of high electron affinity that is often involved as an electron acceptor in charge-transfer complexes.[112] The additional electron in the negative ion enters the LUMO, which is the π^* orbital of ethylene lowered by conjugation with the electron-withdrawing CN groups. The ETE value,[43] EA = 3.17 eV, is much higher than the electron photodetachment value of Lyons,[114] 2.3 eV. The photodetachment threshold curve had no visible structure above the onset which occurred at 2 eV.[114] Lyons and Palmer, realizing that an EA value of 2 eV is much too low, fitted the threshold curve to an assumed vibrational progression involving transitions from a vibrationally excited negative ion to the ground state of the neutral and obtained an EA = 2.3 eV. Kebarle[43] has argued that the above analysis, while plausible, need not be true and that higher vibrational excitation in the ion may have been present. The ETE value[43] (3.17 eV) is in fair agreement with the results from the magnetron method,[115] 2.9 eV, and a value of 2.9 eV derived by Chen and Wentworth[116] on the basis of charge-transfer spectra in solution (see Table II). Lindholm,[117] in his compilation of EA values obtained with the semiempirical HAM/3 method, also obtains a value of 2.9 eV. The values that cluster at 2.9 eV are not necessarily very accurate or reliable. For example, the solution-derived values[116] for compounds with high EA are too low because they neglect decreasing solvation of the resulting strongly charge delocalized anions (see section VI). Thus the ETE value of ~3.1 eV is probably the best value.

V. Entropy Changes on Electron Attachment, ΔS_a°

The entropy changes for electron-transfer equilibria ΔS_1°, obtained[38,41-46] from van't Hoff plots of the equilibrium constants K_1, can be combined in a ΔS_1° scale. Calibration of the scale to the electron attachment entropy for SO_2 $\Delta S_a^\circ(SO_2)$, calculated from the known geometries and vibrational frequencies of SO_2 and SO_2^-, leads to absolute values ΔS_a°(B) for all compounds B that are part of the ΔS scale. This procedure was discussed in greater detail in section II. It should be recalled that the stationary electron convention was adopted, such that ΔS_a° does not include the loss of translational entropy of the electron.

$$A + e = A^- \qquad \Delta S_a^\circ$$

A partial ΔS_a° scale was shown in Figure 6. Representative ΔS_a° values obtained with the ETE method are given in Table III. Kebarle et al.[41] have estimated an average error of $\pm$2 cal/K for the ΔS_a° determinations.

TABLE III. Entropy of Electron Attachment $\Delta S_a°$ for Some Representative Molecules[a]

molecule	$\Delta S_a°$
SO_2[b]	2.0
NO_2[b]	−0.8
$C_6H_5NO_2$[b]	−1.0
2-$CH_3C_6H_4NO_2$[b]	−1.6
4-$CNC_6H_4NO_2$[b]	−2.7
4-$NO_2C_6H_4NO_2$[b]	−4.5
$C_6H_4O_2$ (*p*BQ)[b]	−4.0
$C_{10}H_6O_2$ *p*(NpQ)[b]	−4.0
1-$NO_2C_{10}H_7$ (1-nitronaphthalene)[c]	−0.9
1-$CHOC_{10}H_7$ (1-naphthaldehyde)[c]	3.7
C_6F_6[d]	7.4
C_6F_5CN[d]	4.4
$C_{10}H_8$ (azulene)[c]	4.5
SF_6[b,f]	13.0
C_7F_{14}[b]	2.5
$C_{14}H_{10}$ (anthracene)[c]	−1.3
9-$NO_2C_{14}H_9$ (9-NO_2-anthracene)[c]	−2.9
9-$CHOC_{14}H_9$ (9-CHO-anthracene)[c]	−2.7
4-$CF_3C_6H_4CN$ (4-CF_3-cyanobenzene)[e]	2.6
4-CNC_6H_4CN (4-CN-cyanobenzene)[e]	2.0

[a] $\Delta S_a°$ in cal/K for reaction: e + B = B^-, stationary electron convention. Estimated error in determinations ±2 cal/K. $\Delta S_a°$ are taken from the references as follows: (*b*) ref 41; (*c*) ref 45; (*d*) ref 42; (*e*) ref 43; (*f*) $\Delta S_a°(SF_6)$ in ref 41 is shown to be +18.0 cal/K; due to a misprint, it should read +13.0 cal/K.

On the whole (see Figure 6), most of the absolute values for $\Delta S_a°$ are relatively small, i.e., less than 3 cal/K. This means that for a temperature of 300 K the $T\Delta S_a°$ term amounts to less than 1 kcal/mol, so that the $\Delta G_a°$, $\Delta H_a°$, and −EA values, for most compounds, are within ±2 kcal/mol or ±0.1 eV of each other (see section II).

All compounds examined, except NO_2, have electronic singlet states for the neutral molecule, which become doublets due to the entrance of a single electron in the LUMO on formation of the negative ion. For these the $\Delta S_a°$(electronic) = R ln 2 = +1.4 cal/degree. For NO_2, the reverse is the case, such that the change due to multiplicity is −1.4 cal/degree. The observed $\Delta S_a°$ generally include also other larger contributions. Large $-\Delta S_a°$ values correspond to considerable loss of freedom due to stiffer internal motions or due to increased symmetry (order) of the anion. For large positive $\Delta S_a°$ the converse will be true; i.e., the internal motions in the anion are relatively looser and/or the anion symmetry is lower than that of the neutral.

The substituted nitrobenzenes[41] are found to have negative $\Delta S_a°$. The $-\Delta S_a°$ increase with multiple NO_2 substitution. Thus singly NO_2-substituted benzenes have $\Delta S_a° \approx -1$ to −2 cal/K, while dinitrobenzenes are close to −4 cal/K (Table III).

Kebarle et al.[41] assumed that the negative $\Delta S_a°$ values for the nitrobenzenes are due to stiffening internal rotation of the NO_2 groups due to increased π density in the C–N bond of the anions. Additional stiffening of the O–N–O bending vibrations in the anion was also invoked.[41] The quinones, which also have negative $\Delta S_a°$ values, also must have stiffer anions.[41]

The cyanobenzenes like 4-CF_3 cyanobenzene and 4-CN cyanobenzene have small positive $\Delta S_a°$ values (Table III). The CN group, being colinear with the aromatic carbon atom in the ipso position, does not exhibit internal rotation, and the absence of stiffening of such a rotation in the negative ion could be responsible for the observed $\Delta S_a°$ values.[41,43] Furthermore, the CN group withdraws fewer π electrons than NO_2 or CHO and has fewer vibrations that will stiffen with negative charging.[41,43]

Larger positive $\Delta S_a°$ values are observed for the perfluorobenzenes and particularly for perfluorobenzene itself, which has $\Delta S_a°$ = 7.4 cal/K (Table III). The negative charge on the electronegative F atoms combined with the negative character of the aromatic ring in the negative ion probably weakens the C–F bonds in the negative ion and loosens the C–F vibrations. For $C_6F_6^-$ the resulting positive $\Delta S_a°$ is probably further increased by the loss of symmetry occurring for the change from C_6F_6 to $C_6F_6^-$. The symmetry of $C_6F_6^-$ is not exactly known but is expected[42,92,93] to be much lower than the D_{6h} symmetry of C_6F_6.

The largest positive entropy change, $\Delta S_a°$ = 13 cal/K, was observed[38] for SF_6. The loosening of the S–F bonds in SF_6^- predicted by the theoretical calculation of Hay[70] can explain, together with $\Delta S_a°$(electronic), at most $\Delta S_a° \approx +9$ cal/K. The higher experimental value of 13 cal/K may be due to experimental error, which for the slow SF_6 electron-transfer kinetics[38] may be larger than usual. Another possibility[38,94] is that the geometry of SF_6^- is not that of a regular octahedron but of a structure[94] resembling SF_5^-·F, which is not only looser but also has a much lower symmetry than SF_6.

VI. Solvation Energies of Anions A^- and Binding Energies in A^-·B Complexes

A. Solvation Energies of Anions from Polarographic Half-Wave Potentials. Relationship to Gas-Phase Solvation

Information on the energies of radical anions formed in solution can be obtained from the spectroscopic transitions of charge-transfer complexes[15-18] or from polarographic half-wave potentials $E_{1/2}$. More abundant data are available for the half-wave potentials, and therefore this review will restrict the discussion to these results.

The relationship[118-121] between one electron reversible polarographic half-wave potentials $E_{1/2}$ and the gas-phase electron affinity is given in eq 14. $\Delta G_a°$ is the

$$E_{1/2}(A) = -\Delta G_a°(A) - \delta\Delta G_{solv}°(A^-) + \text{const} \quad (14)$$

$$\delta\Delta G_{solv}°(A^-) = \Delta G_{solv}°(A^-) - \Delta G_{solv}°(A) \quad (15)$$

free energy for the gas-phase electron attachment reaction: e + A = A^- (see eq 4). Since $\Delta G_a°$ were not generally available prior to the ETE measurements, the approximation EA ≈ $-\Delta G_a°$ was made. The value of the constant in (14) depends on the nature of the reference half-cell used in the measurement.

Relationship 14 was used[116,118] for evaluation of gas-phase EA from available $E_{1/2}$. Thus, Wentworth et al.[116] assumed that $\delta\Delta G_{solv}°(A^-)$ does not change for different A. This term can then be included in the constant and (14) reduces to (16). Adjusting the value of the con-

$$E_{1/2}(A) = \text{EA}(A) - \text{const} \quad (16)$$

stant so as to obtain agreement with some known electron affinities in the gas phase, Wentworth et al.[116] were able to predict a large number of EA values. This

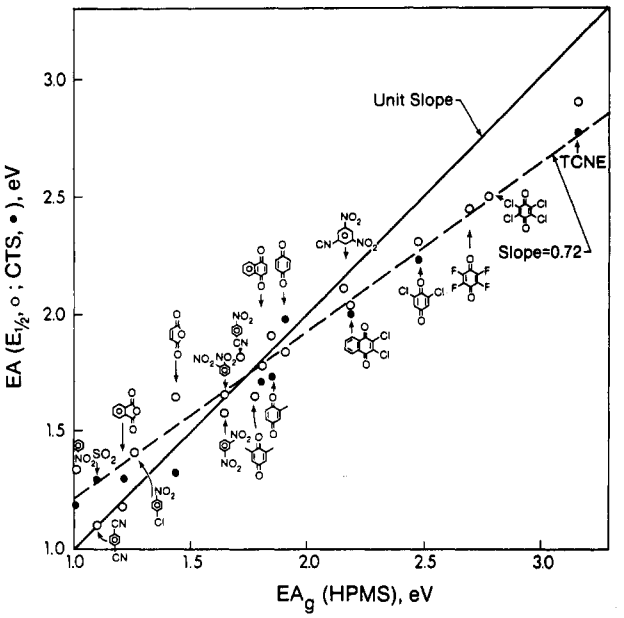

Figure 13. Plot of gas-phase electron affinities from electron-transfer equilibria measurements vs. electron affinities deduced from polarographic half-wave potentials (see eq 16) and charge-transfer spectra by Chen and Wentworth.[116] Observed slope is not equal to 1 but is ≈0.72. This reveals the effect of decreasing solvation exothermicity with increasing charge delocalization of negative ions since high EA molecules lead to ions with more extensive charge delocalization. From Grimsrud.[37]

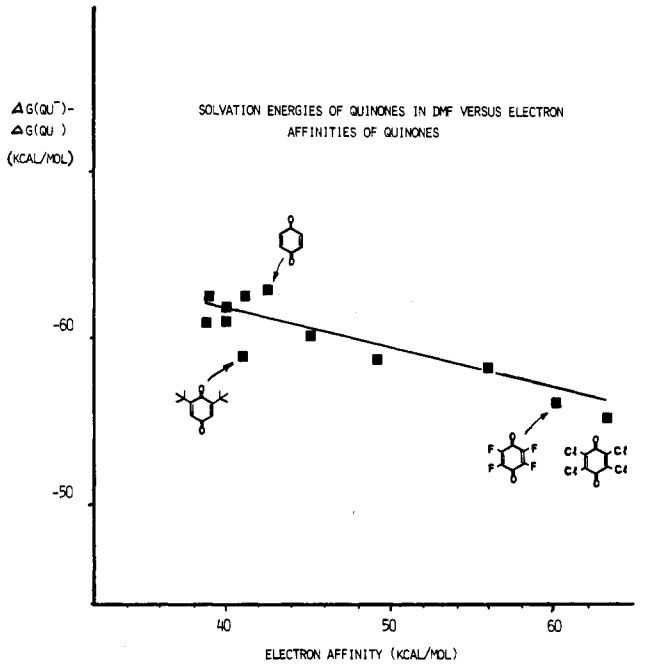

Figure 14. Solvation energies of quinones Q vs. electron affinities: $-\Delta G_a°(Q) \approx EA(Q)$. Solvation energies $\Delta G_s°(A^-) - \Delta G_s°(A)$, in dimethylformamide, where A = Q were obtained from polarographic half-wave potentials (see eq 17) and gas-phase ETE measurements of electron affinities. From Heinis.[46a]

work was done before abundant EA values due to ETE measurements became available.

A plot of EA(A) values obtained from (16) vs. $-\Delta G_a°(A) \approx EA(A)$ values obtained from ETE measurements[37] is shown in Figure 13. While an approximately linear relationship is obtained over a given range, the slope of the line is not equal to unity but is smaller (≈0.72). Further comparisons[45,46a] of ETE data with $E_{1/2}$ values showed that the slope is also solvent dependent. The effect is due[37,45,46] to the neglect of $\delta\Delta G_{solv}°(A^-)$ in eq 16. The solvation difference $\delta\Delta G°(A^-)$ is dominated by the solvation of the anion $\Delta G_{sol}°(A^-)$, and an approximate linearity of $E_{1/2}$ with EA means that the $-\Delta G_{sol}(A^-)$ decreases approximately in proportion with the increase of electron affinity.[37] Higher electron affinity for the compounds shown in Figure 13 is achieved by increased substitution with electron-withdrawing groups, and this leads to increased charge delocalization in the anion. It has long been known that an increase of charge delocalization leads to a decrease of ion solvation.

The availability of EA and $\Delta G_a°$ from ETE measurements made it possible to obtain approximate[45,46] solvation energies $\delta\Delta G°(A^-)$ from half-wave potentials. Heinis et al.[45,46] used eq 17, which follows from (14) and

$$-\delta\Delta G_{solv}°(A^-) = \Delta G_a°(A) + E_{1/2}(A) - 4.99 \text{ eV} \quad (17)$$

contains the absolute value of the standard calomel electrode against which the $E_{1/2}$ values were measured. All values in (17) are in electronvolts. Some of the results obtained[46] for the quinones are shown in Figure 14.

The $\delta\Delta G_{sol}°(A^-)$ term is dominated by the solvation of the anion, since the solvation of the neutral is expected to be only a few kilocalories per mole. Thus, the $\delta\Delta G_{solv}°(A^-)$ values can be taken to essentially represent the solvation of the anion.[45,46] The approximately linear decrease of solvation exothermicity with increasing electron affinity of the quinones can be clearly seen in Figure 14. Some compounds show larger deviations from linearity. Thus the 2,6-bis(*t*-Bu)-*p*-BQ anion shows significantly lower solvation exothermicity (see Figure 14). The lower exothermicity was attributed[46] to steric hindrance exerted by the *t*-Bu groups for the specific solvation of the negative charge center of the O atom in position 1.

Solvation energies for substituted benzenes, naphthalenes, and anthracenes obtained by a similar procedure by Heinis et al.[45] are also available. It was also shown that the solvation exothermicity ($-\Delta G_{solv}°(A^-)$) decreases faster with increasing charge delocalization in A^- for protic solvents (methanol) relative to dipolar aprotic solvents like dimethylformamide and acetonitrile.[45]

B. Binding Energies in A^-·Sl Complexes

The solvation energies in a given substituted ion series are often found to be parallel to the "solvation" trends observed when the ions are solvated by only one or a few solvent molecules. Chowdhury et al.[46b] measured the gas-phase equilibria (eq 18) where A^- were

$$A^- + Sl = A^-·Sl \quad (18)$$

substituted nitrobenzene radical anions and Sl were the solvent molecules methanol, acetonitrile, dimethylformamide, and dimethyl sulfoxide. They found that the $-\Delta G_{18}°$ for a given Sl decrease as the electron affinity of A increases, i.e., as the charge delocalization in A^- increases. Some of these results are shown in Figure 15. This effect parallels the decrease of $-\Delta G_{solv}°(A^-)$ with charge delocalization observed for liquid solvents (see Figure 14). Furthermore, the decrease observed for the dipolar aprotic acetonitrile molecule was found[46b] to be smaller than that for the

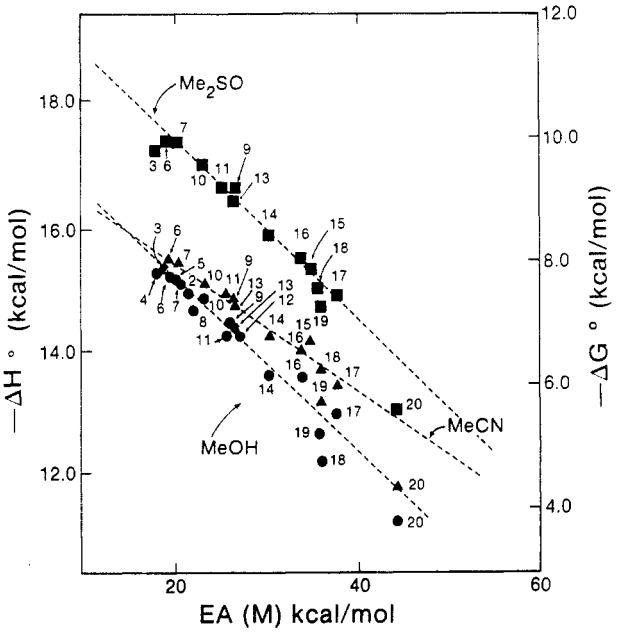

Figure 15. Plot of $\Delta G°$ at 70 °C and $\Delta H°$ for the reactions A^- + Sl = A^-·Sl vs. electron affinity of A. The three plots are for Sl = dimethyl sulfoxide (Me_2SO), acetonitrile (MeCN), and methanol (MeOH). The actual A^- are identified by the number. All A^- used in the plot were substituted nitrobenzenes (XNB). Substituent X: (1) 2,3-diCH_3; (2) 3-OCH_3; (3) 4-OCH_3; (4) 2-CH_3; (5) 3-CH_3; (6) 4-CH_3; (7) H; (8) 2-F; (9) 3-F; (10) 4-F; (11) 2-Cl; (12) 3-Cl; (13) 4-Cl; (14) 3-CF_3; (15) 2-CN; (16) 3-CN; (17) 4-CN; (18) 2-NO_2; (19) 3-NO_2; (20) 4-NO_2. Decrease of exothermicity with increase of electron affinity attributed to increasing charge delocalization in anion A^- with increasing EA(A). From Chowdhury.[46b]

protic methanol molecule (see Figure 15), an effect occurring also with the respective liquid solvents. Chowdhury et al.[46b] attributed the greater decrease of solvation with charge delocalization observed for protic relative to dipolar aprotic molecules to the detailed distribution of the net atomic charges constituting the dipole of the two types of solvent molecules. In the dipolar aprotic CH_3CN the dipole is located mostly on the C^+N^- group which is relatively distant from the A^- in the A^-·CH_3CN complex. The distant location of the dipole results in a lesser decrease of the binding energy in A^-·CH_3CN with increasing charge delocalization in A^-. For protic solvents the dipole RO^-H^+ can approach the negative ion very closely, and this close approach leads to a strong decrease of the interaction when the charge delocalization is increased. The situation is analogous to solvation by protic and aprotic solvents observed[122] for other negative ions like Cl^-, Br^-, and I^-.

C. Binding Energies in A^-·B Complexes

In this section, we will consider information available on the stabilities of A^-·B complexes. In a narrow sense A and B are the compounds engaged in the electron-transfer reaction (eq 1), i.e., compounds whose electron affinities are given in Table II. However, as pointed out the preceding section, stabilities of complexes where the neutral molecule is a solvent molecule (B = Sl) are also of interest from the standpoint of the solvation of the radical anions A^- and electron transfer in solution. Another extension of the type of ion–neutral complexes considered comes about from the desire to understand the bonding in A^-·B. When both A and B are compounds of the type included in Table II, i.e., substituted

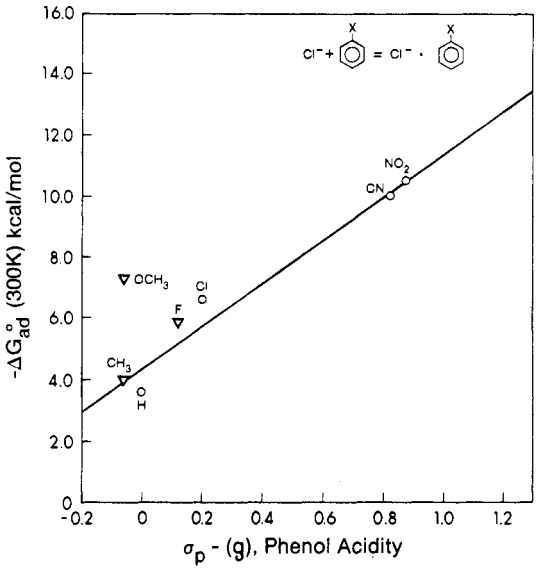

Figure 16. Free energy changes for adduct formation Cl^- + C_6H_5X = Cl^-·C_6H_5X vs. substituent parameter σ_p- of Taft,[75] based on gas-phase phenol acidities. σ_p- increase approximately in proportion with electron affinities of C_6H_5X: (○) data from Chowdhury;[46b,124] (△) data from French.[123]

aromatics, quinones, etc., one deals with a somewhat complex situation because of the complexity of A and B. It is easier to examine bonding in ion–neutral adducts where the structure of either the ion or the neutral is relatively simple. Therefore ion–neutral complexes will also be considered where only the ion or the neutral is a compound from Table II, i.e., a substituted aromatic compound or a quinone, etc.

Early PHPMS measurements and interpretation by French et al.[123] dealing with the complexes Cl^-·B, where B are substituted benzenes, were recently extended by Chowdhury et al.[72] to a wider variety of benzenes. The binding energies were found to increase with the electron affinity of the substituted benzenes. A plot of these data is shown in Figure 16. An increase of binding energies with increasing electron affinity of B was also observed[40] for the adducts NO_2^-·B, where B were substituted benzenes and quinones (see Figure 17).

Finally, an approximately linear relationship was observed between the binding energies in NO_2^-·B adducts and the binding energies of 1,2-$C_6H_4(NO_2)_2^-$·B adducts[124] (Figure 18). The last relationship also means that the 1,2-$C_6H_4(NO_2)_2^-$·B binding energies increase approximately linearly with EA(B). The relationship between the binding energies and the electron affinity of B was assumed[40,72,124] to be indirect. Following the initial interpretation of French et al.,[123] which was supported by theoretical calculations,[123] the stabilization energy in the adducts was assumed to be due to hydrogen bonding. This is illustrated by structure VIII.

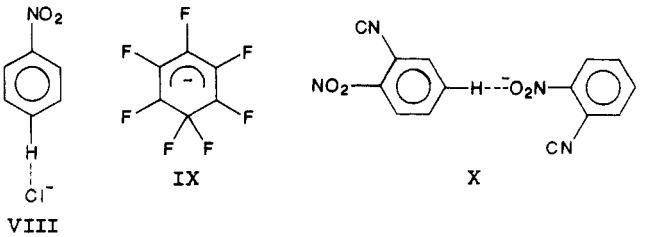

The partially positive character of the benzene hydrogens is increased by the π withdrawal and –I field effect

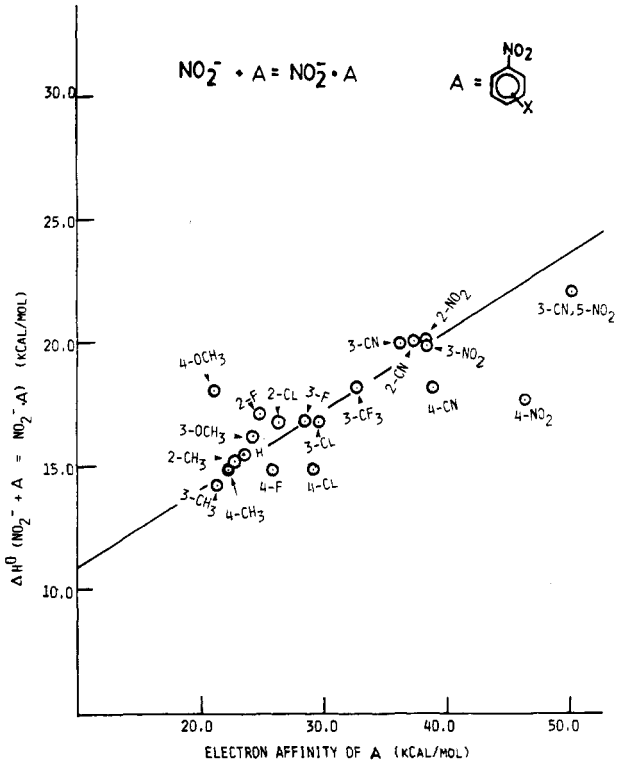

Figure 17. Plot of enthalpy change for reaction NO_2^- + B = NO_2^-·B vs. electron affinity of B. Compounds B are substituted nitrobenzenes. Substituent and position of substituent indicated on plot. Data from Grimsrud.[40]

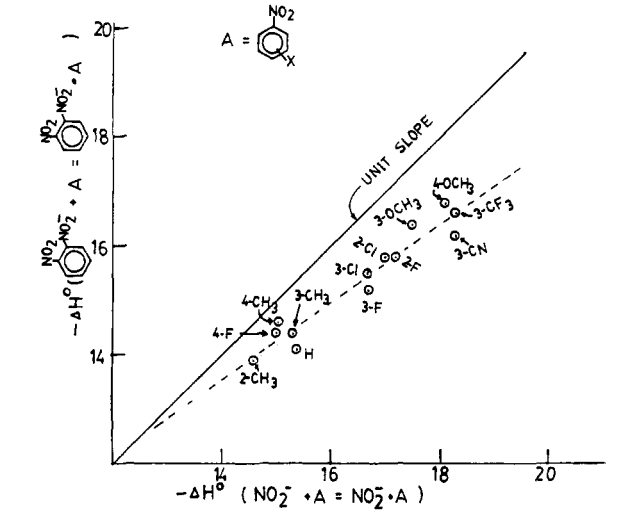

Figure 18. Plot of enthalpy change for the reaction 1,2-$C_6H_4(NO_2)_2^-$ + B = 1,2-$C_6H_4(NO_2)_2^-$·B vs. enthalpy change for NO_2^- + B = NO_2^-·B, where B are substituted nitrobenzenes. Data from Grimsrud[40] and Chowdhury.[72,124]

of the electron-withdrawing groups (NO_2, CN, etc.). This strengthens the hydrogen bond to Cl^-. Increase of electron affinity of the benzene is achieved by increased substitution with electron-withdrawing groups, but these groups also increase the positive character of the hydrogens in the substituted neutral benzene.

Benzenes substituted with a number of electron-withdrawing groups are known,[125] from experiments in solution, to form σ complexes (Meisenheimer complexes) with a number of anions like the hydroxy and alkoxy anions and also with SO_3^-, F^-, etc. The Meisenheimer complexes[125] are an interesting field of research in organic chemistry because of their special bonding and their presumed role in nucleophilic aromatic substitution (S_NAr). Since even thioethoxide anions can form Meisenheimer complexes[125] the question can be asked whether some of the A^-·B complexes observed in the gas phase and discussed above do have the σ complex structure. A recent study of Hiraoka et al.[126] reported the observation of the Meisenheimer type complex of F^- with C_6F_6 (structure IX). The bond energy F^-–C_6F_6 was obtained[126] by a van't Hoff plot of the equilibrium constant for the gas-phase reaction (eq 19)

$$F^- + C_6F_6 = F^-\cdot C_6F_6 \text{ (IX)} \qquad (19)$$

$$\Delta G_{300K}^\circ = -20.4 \text{ kcal/mol}$$

$$\Delta H^\circ = -27.5 \text{ kcal/mol}$$

studies with PHPMS apparatus. Structure IX was predicted from 3-21G ab initio MO calculations.[126] The two equivalent fluorines were found to have C–F bond distances of 1.403 Å, while the other five C–F bonds had shorter, 1.368 Å, bond lengths. Hiraoka et al.[126] obtained also a structure for $F^-\cdot C_6H_6$ predicted by calculation. This is the hydrogen-bonded structure VIII. Thus, as expected, the presence of strongly electron withdrawing groups on the aromatic ring is essential for the formation of the σ complex.

The formation of Meisenheimer complexes in solution is adversely affected by the significantly lower solvation energy of the large Meisenheimer complex negative ion relative to the large solvation energy of the small nucleophile X^-. In the gas phase this effect is absent. Thus bond-energy determination of even weakly bonded σ complexes should be possible with the PHPMS ion–adduct equilibria technique.

Among the adducts appearing in Figures 16–18, the only species that could have Meisenheimer σ complex structures are the NO_2^-·B species, where B are benzenes with very high electron affinities, i.e., multiply substituted with electron-withdrawing groups. Experimental measurements of adduct equilibria involving stronger nucleophiles like F^-, OH^-, and alkoxy$^-$ ions are presently under way in the reviewer's laboratory.

Sieck[127] has also reported recent studies of bonding of NO_2^- and $C_6H_5NO_2^-$ to several polar molecules. This work was based on measurements of the adduct formation equilibria with a PHPMS instrument. In general, the conclusions reached by Sieck are similar to those described above and in section VI.B.

Adduct A_2^- bond energies obtained from equilibria measured[124] with PHPMS are given in Figure 19. The A_2^- binding energies showed[124] no correlation with the electron affinity of A. The plot in Figure 19 demonstrates that there is an approximately linear increase of A^-–A binding energy with the dipole moment of A. The 4-NO_2 and particularly 4-CN nitrobenzenes are important exceptions. These have substantial binding energies but no molecular dipole due to cancellation of the opposing C–NO_2 group dipoles. These exceptions suggest that the presence of a net molecular dipole is only one factor favoring bonding. Since the binding energies plotted in Figure 19 are all for substituted nitrobenzenes, the polarizabilities of all A(X–NB) molecules will be similar. The interaction of the negative ion with the polarizability of the neutral molecule could also be a factor favoring bonding. This interaction will be similar for all cases shown in Figure 19. The

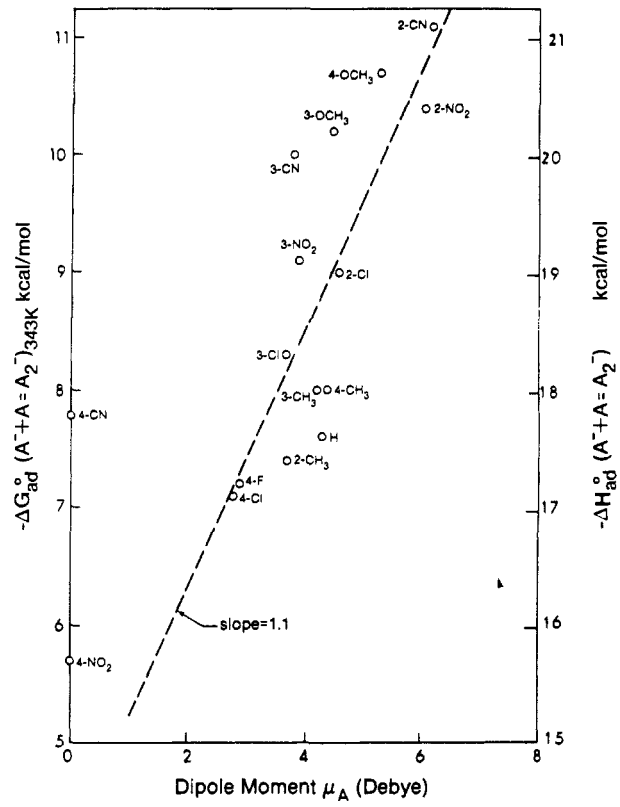

Figure 19. Binding free energies for adduct formation $A^- + A = A_2^-$ vs. dipole moment of A. From Chowdhury.[124]

hydrogen-bonded structure type X was suggested[124] for the A_2^- nitrobenzene adducts. Structure X shows the most strongly bonded A_2^- among the compounds in Figure 19. The π withdrawal and the dipole field effect in the neutral 2-CN nitrobenzene are assumed to increase the protic character of the hydrogen entering the H bond with the negative ion.

The bonding in adducts $Cl^-\cdot SF_6$, $SF_6^-\cdot A$, and $Cl^-\cdot C_6F_6$ was studied[38] in connection with the electron-transfer kinetics involving SF_6^- and A (where A are substituted nitrobenzenes and quinones) and are shown in structures XI and XII (for kinetics see section III). It was

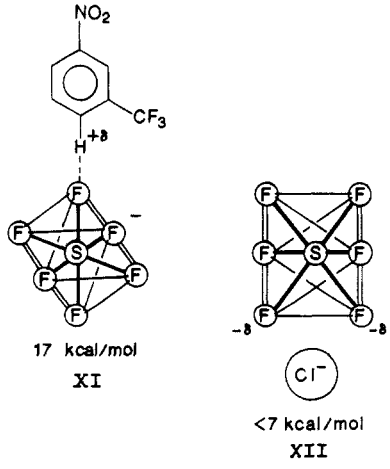

found that extremely weakly bonded adducts are formed between Cl^- and SF_6. This was attributed[38] to the dodecapole in SF_6. The strong electronegativity of the fluorine atom leads to a substantial negative charge on the F atoms in SF_6, and this leads to weak bonding to the negative Cl^- (structure XII). Similarly weak bonding is expected for adducts of SF_6 with any other negative ions of similar or larger size than Cl^-. The bonding observed[38] for $Cl^-\cdot C_6F_6$ was very much stronger than that for $Cl^-\cdot SF_6$. This was surprising since from an electrostatic standpoint SF_6 and C_6F_6 are similar, i.e., both expose a negatively charged surface to the negative ion. In C_6F_6 this negative surface includes the π clouds. However, the existence of the strongly bonded Meisenheimer type complex for $F^-\cdot C_6F_6$ indicated by Hiraoka's work[126] suggests that the binding in $Cl^-\cdot C_6F_6$ may bear some similarity to that in $F^-\cdot C_6F_6$ (structure IX). One would expect that the C–Cl "bond" will be considerably longer than the C–F bond in the ipso position.

The relatively strong bonding observed in $SF_6^-\cdot B$ was attributed[38] to hydrogen bonding between B and one of the (negatively charged) F atoms in SF_6^- (see structure XI).

VII. Thermal Stability of Anions: Electron Attachment and Detachment at Thermal Energies

The formation of anions B^- by electron capture and the thermal stability of B^- with respect to thermal electron detachment (autodetachment) depend on the values of the attachment and detachment rate constants k_a and k_d, which in turn define the attachment–detachment equilibrium constant K_a as shown in eq 20 and 21. Christophorou[95] has discussed the factors

$$e + B \rightleftarrows B^{-*} \xrightarrow{M} B^- \quad (20)$$

$$e + B \underset{k_d}{\overset{k_a}{\rightleftharpoons}} B^- \quad (21)$$

$$K_a = \frac{k_a}{k_d} = \frac{\exp(\Delta S_a^\circ/R)\,\exp(-\Delta H_a^\circ/RT)}{Q_{e^-}} \quad (22)$$

$$k_d = 4.8 \times 10^{15} T^{3/2} k_a \exp[-\Delta S_a^\circ/R - EA/RT] \quad (23)$$

$$\Delta H_d^\circ = -\Delta H_a = EA \qquad \Delta S_d^\circ = -\Delta S_a^\circ$$

determining the magnitude of the attachment rate constants k_a. Since the energy, equal to EA(B), released in the attachment must be removed and, conversely, in thermal detachment B^- must be thermally activated, both the attachment and detachment rates are dependent on the presence of third bodies M (see eq 20). Christophorou[95] provides a tabulation of literature values of the limiting, high-pressure, values k_a determined experimentally. Since the lifetimes of the excited ions B^{-*} are generally relatively long[95] ($\tau \gg 10^{-6}$ s), the limiting rates should generally apply at pressures above 1 Torr, i.e., for the PHPMS conditions. Values for k_a are available[95] for substituted benzenes, quinones, and perfluoro compounds, i.e., the compound classes represented in Table II. In general the values are between $k_a \approx 10^{-7}$ and 10^{-9} $cm^3 \cdot molecules^{-1} \cdot s^{-1}$. Most of the k_a are found[95] to be approximately temperature independent in the temperature range 300–600 K. Unfortunately, it appears that there are no simple criteria which could be used to predict the value of k_a. Thus 1,4-benzoquinone has a very low k_a, such that it is barely detectable with PHPMS,[46] while the closely related 1,4-naphthoquinone has a relatively high $k_a = 6 \times 10^{-8}$ $cm^3 \cdot molecules^{-1} \cdot s^{-1}$. Substituted benzoquinones also have[46] relatively high k_a.

Values for the equilibrium constant K_a can be evaluated from the $\Delta G_a°$ determined by the ETE method and given in Table II. Since $K_a = k_a/k_d$, one can evaluate k_d, the detachment rate constant, when k_a values[95] are available (eq 23). Grimsrud et al.[39] were able to obtain experimentally determined values for k_d of azulene. These were obtained by observing with a PHPMS the time dependence of the decay of the azulene negative ion, Az^-, at high temperatures. An electron scavenger was used to capture the electrons released by Az^- and prevent their reattachment to Az. The experimentally determined k_d were found in good agreement with k_d evaluated with eq 23 into which $\Delta S_a°$ and $\Delta H_a°$ from ETE measurements and k_a from Christophorou[95] were substituted.[39]

Equation 23 can be used for determinations of the rate of thermal electron autodetachment from ions B^- for which $\Delta G_a°$ (Table II) and experimental k_a values are available. It turns out that ions B^- with electron affinities of less than 10 kcal/mol autodetach electrons at temperatures above 100 °C with sufficiently high rate so that the decrease of the B^- intensity over 1 ms is very noticeable and its rate generally comparable to the electron-transfer equilibria (eq 1) rates. ETE measurements for compounds with electron affinities less than 10 kcal/mol can be executed only at lower temperatures, but at such low temperatures there is often interference from excessive adduct $(A·B)^-$ formation (see section V.C).

Chen and Wentworth[11,116,128] have used a technique dependent on the thermal electron detachment rates to determine electron affinities. The electron concentrations are determined with a gas chromatographic electron capture detector operated at different temperatures. The technique is well suited for compounds with electron affinities below 20 kcal/mol. For these cases the corresponding negative ions detach electrons at sufficient rates at temperatures where the compounds themselves are thermally stable.

Electron attachment and detachment rates are of importance also in chemical ionization mass spectrometry (see section VIII).

VIII. Relevance of Data to Analytical Mass Spectrometry

Information on ion–molecule reaction rates and energetics is of fundamental importance to analytical mass spectrometry and particularly chemical ionization (CI). The significance of this type of information to CI has been very well brought out by Harrison[4] in his monograph on chemical ionization (see Chapter 2).[4] Recently, the analytical areas to which ion–molecule rates and energetics specifically apply have increased. Thus it is being recognized that relative ion intensities observed in FAB mass spectrometry are strongly affected by gas-phase ion energetics (see papers by R. G. Cooks and C. Fenselau in this issue). Thus, protonated analytes MH^+ are observed only when the matrix compound is of lower proton affinity[129-132] and gas-phase basicities (proton affinities) rather than solution basicities determine the relative intensities of the MH^+ ions of two coanalytes from the same matrix.[133]

The rapidly developing thermospray method,[134] which leads to production of gas-phase ions from analytes present in liquid chromatography effluent, also leads to mass spectra that depend on the energetics of the gas-phase ions desorbed from the microdroplets.[135] Furthermore, these primary thermospray ions subsequently engage in gas-phase ion–molecule reactions.[136]

The most important analyte (M) ions occurring in negative ion chemical ionization[129] (NICI) are M^-, $(M-H)^-$, and adduct ions M_2^- and $X^-·M$, where X^- is a reagent ion, typically a halide anion.[4] Mass spectral analysis, where the analyte ions are primarily detected as M^-, is also called electron capture CI. Very high sensitivities of detection can be achieved[137] with electron capture CI. The high sensitivity is primarily due to the high yield of thermal secondary electrons produced by the primary ionization of the "reagent" gas and subsequent thermalization of the electrons by collisions with the reagent gas. The electron capture rate constants k_a for compounds with positive electron affinities are 1–2 orders of magnitude larger than those for ion–molecule reactions (see section VI), and this is the second important factor contributing to the sensitivity of electron capture CI. A limitation of the technique is that the analytes M must have positive EA. Furthermore the EA(M) should be larger than about 10 kcal/mol. CI sources are operated generally at 150–200 °C, and for these temperatures rapid thermal electron detachment can be expected when EA(M) $\leq$ 10 kcal/mol (see section VI).

The EA data in Table II and Figure 10 and discussion in section IV illustrate well the classes of compounds with sufficiently high EA to be detected as M^- in electron capture CI. While similar data[14,83,128] existed before the ETE measurements were reported, the present compilation containing ETE results is much more extensive, self-consistent, and believed to be more accurate.

Analytes that do not have the required electron affinity can, by derivatization, be provided with groups that do have low lying LUMO's that confer electron affinity to the derivatized analyte. Typical groups introduced through derivatization are $C_6F_5CO^-$ and $NO_2C_6H_4CO^-$. Examination of Table II and particularly the data on the perfluoro and nitrobenzenes together with consideration of the substituent effects (section IV) clearly shows that these groups will confer the desired minimum EA to practically any analyte.

Buchanan et al.[2] and Iida et al.[3] have suggested that two isomeric analytes can be distinguished from one another when one has an EA > 10 kcal/mol and thus can be expected to form M^- while the other has an EA < 10 kcal/mol and thus is not expected to give M^-. Both groups of researchers[2,3] examined NICI of polyaromatic hydrocarbons (PAH's). Unfortunately, the results from the two groups were somewhat contradictory. Buchanan[2] observed M^- for azulene but not for the isomeric naphthalene. This result is to be expected from the data in Table II and Figure 10. Azulene has an EA of 16 kcal/mol, while naphthalene, according to Jordan[73] (see Figure 10), has a negative EA. In the reviewer's laboratory the azulene negative ion was easily produced (see section VI), while the naphthalene negative ion could not be seen. On the other hand, Iida[3] observed M^- for both azulene and naphthalene. Iida's[3] results are clearly anomalous, although the reason for this anomaly is not clear. Buchanan[2] did not observe M^- from anthracene, while in the reviewer's laboratory

this ion was observed and in fact an EA(anthracene) = 13.8 kcal/mol (Table II) was determined.[45] Clearly, the present EA data, even though insufficient to explain exactly what happens in some of the analytical negative ion CI sources, provide a firmer basis for discussion.

An interesting application of data contained in this review deals with the question of whether electrons are created in the matrix on fast atom bombardment. The negative-ion FAB spectrum of 1,4-benzoquinone (1,4-BQ) in a glycerol matrix is very weak[139,140] and contains only a very low intensity of the molecular ion M^-. Clayton[139] assumed that M^- is formed by capture of electrons by 1,4-BQ. Cotter[140] found much higher yields for M^- when sulfolane was used as a matrix. The presence of the 1,4-BQ reduced the intensity of the FAB MS peak m/z 64 from sulfolane, and this was attributed to reaction 24. The SO_2^- was presumed to be produced

$$SO_2^-(m/z\ 64) + \text{1,4-BQ} = SO_2 + \text{1,4-BQ}^- \quad (24)$$

by the heterolytic dissociation of sulfolane induced by the atom impact. A heterolytic dissociation is generally an energetically more favorable process than the formation of a positive ion and an electron. Cotter[140] concluded, in agreement with earlier interpretation by Barber,[141] that electron production by the fast atom impact is not an important process.

The data in Table II show that the electron affinity of SO_2 is lower than that of 1,4-BQ so that reaction 24 is energetically permitted. The kinetics data (see section III) indicate also that reaction 24 is likely to be fast, i.e., proceed at every collision. Thus Cotter's interpretation, on these grounds, is justified. However, in section VI it was pointed out that 1,4-BQ is one of the few compounds with high EA that has a very low electron capture rate constant k_a. Thus 1,4-BQ happens to be one of the few compounds unsuitable for the argument[140] concerning the presence of electrons since even if electrons were present, 1,4-BQ would not have been able to capture them.

$(M-H)^-$ ions are commonly observed in NICI. These ions generally are due to proton abstraction from M by strong gas-phase Bronsted bases like F^-, OH^-, O^-, and Cl^- as shown in reaction 25. The bases are present

$$M + F^- = (M-H)^- + HF \quad (25)$$

either because specific reagents have been added (NF_3 for F^-, CCl_4 for Cl^-, etc.) or are due to chance impurities.[4,142,143] Proton-transfer reactions like (25) will occur under CI conditions only if they are exothermic. The enthalpy and free energy change for a large number of reactions like (25) can be estimated on the basis of available data for the proton affinities of negative ions. These data obtained by measurements of proton-transfer equilibria involving some 300 organic and inorganic acids with PHPMS and ICR apparatuses have been summarized by Bartmess[29,144] and Cumming.[145] The combined use of thermochemical data on electron affinities (Table II) and the acidity data[29,144,145] should represent a very useful and powerful tool for predicting or rationalizing the presence of M^- and $(M-H)^-$ ions in NICI.

Adduct ions are often observed in NICI. These may be dimers of the analyte, i.e., M_2^- or M adducts to specific reagent ions like Cl^- (Dougherty[143]), F^- (Tiernan[146]), etc.[4] The adduct binding energies discussed in section V and quoted in ref 24, 27, 40, 46b, 71, and 123 provide information on a large variety of such complexes. It should therefore be possible on the basis of these data to predict or rationalize the observation of given adducts in NICI and FAB MS.

References

(1) Hunt, D. F.; Stafford, G. C.; Crow, F. W.; Russel, J. W. *Anal. Chem.* **1976**, *48*, 2098.
(2) Buchanan, M. V.; Olerich, G. *Anal. Chem.* **1984**, *19*, 486.
(3) Iida, Y.; Daishima, S. *Chem. Lett.* **1983**, 273.
(4) Harrison, A. G. *Chemical Ionization Mass Spectrometry*; CRC: Boca Raton, FL, 1984.
(5) Clayton, E.; Wakefield, A. J. C. *J. Chem. Soc., Chem. Commun.* **1984**, 969.
(6) Freeman, G. R. *Radiat. Res. Rev.* **1968**, *1*, 1.
(7) Fehsenfeld, F. C.; Schmeltekopf, A. L.; Schiff, H. I.; Ferguson, E. E. *Planet. Space Sci.* **1967**, *15*, 373.
(8) Loeb, L. B. *Basic Processes in Gaseous Elecronics*; University of California: Los Angeles, 1961; p 375.
(9) Lovelock, J. E. *Nature (London)* **1961**, *187*, 49.
(10) Lovelock, J. E. *Anal. Chem.* **1963**, *35*, 474.
(11) (a) Wentworth, W. E.; Chen, E. C. M. *J. Chromatogr.* **1979**, *186*, 99. (b) Wentworth, W. E.; Kao, L. W.; Backer, R. S. *J. Phys. Chem.* **1975**, *79*, 1161.
(12) *Gas Phase Ion Chemistry*; Bowers, M. T., Ed.; Academic: New York, 1979; Vol. 1–3.
(13) Rich, P. R. *Faraday Discuss. Chem. Soc.* **1982**, *74*, 3183.
(14) Christophorou, L. G. *Adv. Electron. Electron Phys.* **1978**, *46*, 55.
(15) Szwarc, M. *Prog. Phys. Org. Chem.* **1968**, *6*, 323.
(16) Biergleb, G. *Angew. Chem., Int. Ed. Engl.* **1964**, *3*, 617.
(17) Eberson, L. *Adv. Free Radical Biol. Med.* **1975**, *1*, 19.
(18) Sutin, N. *Prog. Inorg. Chem.* **1983**, *30*, 442.
(19) Kerber, R. C.; Urry, G. W.; Kornblum, N. *J. Am. Chem. Soc.* **1964**, *86*, 3904; **1965**, *87*, 3420. Eberson, L. *Adv. Phys. Org. Chem.* **1982**, *18*, 79.
(20) Christodoulides, A. A.; McCorkle, D. L.; Christophorou, L. G. *Electron Molecule Interactions and Their Applications*; Academic: New York, 1984; Vol. 2, pp 423–641.
(21) Mead, R. D.; Stevens, A. E.; Lineberger, W. C. In *Gas Phase Ion Chem.* **1984**, *3*, 214.
(22) Drazaic, P. S.; Marks, J.; Brauman, J. I. *Gas Phase Ion Chem.* **1984**, *3*, 168.
(23) Hogg, A. M.; Kebarle, P. *J. Chem. Phys.* **1965**, *43*, 449.
(24) Kebarle, P. *Annu. Rev. Phys. Chem.* **1977**, *28*, 495.
(25) Bowers, M. T.; Aue, D. H.; Webb, H. M.; McIver, R. T. *J. Am. Chem. Soc.* **1971**, *93*, 4314.
(26) Fehsenfeld, F. C.; Ferguson, E. E. *J. Chem. Phys.* **1973**, *59*, 6272.
(27) Castleman, A. W.; Keesee, R. G. *Chem. Rev.* **1986**, *86*, 589.
(28) Lias, S. G.; Liebman, J. F.; Levin, R. D. *J. Phys. Chem. Ref. Data* **1985**, *13*, 695.
(29) Bartmess, J. E.; McIver, R. T. *Gas Phase Ion Chem.* **1979**, *2*, 88.
(30) Sharma, R. B.; Sen Sharma, D. K.; Hiraoka, K.; Kebarle, P. *J. Am. Chem. Soc.* **1985**, *107*, 3797.
(31) McIver, R. T.; Fukuda, E. K. *Lect. Notes Chem.* **1982**, 164.
(32) Fukuda, E. K.; McIver, R. T. *J. Chem. Phys.* **1982**, *77*, 4942.
(33) Fukuda, E. K.; McIver, R. T. *J. Phys. Chem.* **1983**, *87*, 2993.
(34) Fukuda, E. K.; McIver, R. T. *J. Am. Chem. Soc.* **1985**, *107*, 2291.
(35) Grabowski, J. J.; Van Doren, J. M.; DePuy, C. H.; Bierbaum, V. M. *J. Chem. Phys.* **1984**, *80*, 575.
(36) Caldwell, G.; Kebarle, P. *J. Chem. Phys.* **1984**, *80*, 577.
(37) Grimsrud, E. P.; Caldwell, G.; Chowdhury, S.; Kebarle, P. *J. Am. Chem. Soc.* **1985**, *107*, 4627.
(38) Grimsrud, E. P.; Chowdhury, S.; Kebarle, P. *J. Chem. Phys.* **1985**, *83*, 1059.
(39) Grimsrud, E. P.; Chowdhury, S.; Kebarle, P. *J. Chem. Phys.* **1985**, *83*, 3983.
(40) Grimsrud, E. P.; Chowdhury, S.; Kebarle, P. *Int. J. Mass Spectrom. Ion Processes* **1986**, *68*, 57.
(41) Chowdhury, S.; Heinis, T.; Grimsrud, E. P.; Kebarle, P. *J. Phys. Chem.* **1986**, *90*, 2747.
(42) Chowdhury, S.; Grimsrud, E. P.; Heinis, T.; Kebarle, P. *J. Am. Chem. Soc.* **1986**, *108*, 3630. Chowdhury, S.; Nicol, G.; Kebarle, P. *Chem. Phys. Lett.* **1986**, *127*, 130.
(43) Chowdhury, S.; Kebarle, P. *J. Am. Chem. Soc.* **1986**, *108*, 5453.
(44) Chowdhury, S.; Heinis, T.; Kebarle, P. *J. Am. Chem. Soc.* **1986**, *108*, 4662.
(45) Heinis, T.; Chowdhury, S.; Kebarle, P. *J. Am. Chem. Soc.*, submitted.
(46) (a) Heinis, T.; Chowdhury, S.; Scott, S.; Kebarle, P. *J. Am. Chem. Soc.*, submitted. (b) Chowdhury, S.; Grimsrud, E. P.; Kebarle, P. *J. Phys. Chem.*, in press.
(47) Chowdhury, S.; Kebarle, P., unpublished results.

(48) Kebarle, P. In *Techniques of Chemistry*, Saunders, W., Ed.; Wiley: New York, 1987.
(49) Cellota, R. J.; Bennet, R. A.; Hall, J. L. *J. Chem. Phys.* **1974**, *60*, 1740.
(50) (a) Hughes, B. M.; Lifshitz, C.; Tiernan, T. O. *J. Chem. Phys.* **1973**, *59*, 3162. (b) Lifshitz, C.; Tiernan, T. O.; Hughes, B. M. *J. Chem. Phys.* **1973**, *59*, 3182.
(51) Refay, K. M. A.; Franklin, J. L. *J. Chem. Phys.* **1976**, *65*, 1994.
(52) Feldman, D. *Z. Naturforsch., A: Astrophys., Phys. Phys. Chem.* **1970**, *A25*, 621.
(53) Rothe, E. W.; Tang, S.; Reck, G. P. *J. Chem. Phys.* **1972**, *62*, 3829.
(54) Massey, H. S. W.; Burhop, E. H. S. *Electronic and Impact Phenomena*; Oxford University: London, 1962; p 514.
(55) Rapp, D.; Francis, E. W. *J. Chem. Phys.* **1962**, *37*, 2631.
(56) Futrell, J. H.; Tiernan, T. O. In *Fundamental Processes in Radiation Chemistry*; Ausloos, P., Ed.; Wiley: New York, 1968; p 188.
(57) Lindholm, E. In *Ion Molecule Reactions*; Franklin, J. L., Ed.; Plenum: New York, 1972; p 460.
(58) Bohme, D. K.; Hasted, J. B.; Ong, P. P. *J. Phys.* **1968**, 871. *Chem. Phys. Lett.* **1967**, *1*, 259.
(59) Laudenslager, J. B.; Huntress, W. T.; Bowers, M. T. *J. Chem. Phys.* **1974**, *61*, 4600.
(60) Freeman, G. G.; Harland, P. W.; McEwen, M. J. *Chem. Phys. Lett.* **1979**, *64*, 596.
(61) Gioumousis, G.; Stevenson, D. P. *J. Chem. Phys.* **1958**, *29*, 294.
(62) Bass, L.; Su, T.; Chesnavitch, W. J.; Bowers, M. T. *Chem. Phys. Lett.* **1975**, *34*, 119.
(63) Dunkin, D. B.; Fehsenfeld, F. C.; Ferguson, E. E. *Chem. Phys. Lett.* **1972**, *15*, 257.
(64) Fehsenfeld, F. C. *J. Chem. Phys.* **1971**, *54*, 438.
(65) Streit, G. E. *J. Chem. Phys.* **1982**, *77*, 826. Babcock, L. M.; Streit, G. E. *J. Chem. Phys.* **1981**, *75*, 3864.
(66) Olmstead, W. N.; Brauman, J. I. *J. Am. Chem. Soc.* **1977**, *99*, 4219. Farneth, W. E.; Brauman, J. I. *Ibid.* **1976**, *98*, 7891.
(67) Hiraoka, K.; Kebarle, P. *J. Chem. Phys.* **1975**, *63*, 394. Sen Sharma, D. K.; Kebarle, P. *J. Am. Chem. Soc.* **1982**, *104*, 19. Caldwell, G.; Magnera, T. F.; Kebarle, P. *J. Am. Chem. Soc.* **1984**, *106*, 959. Magnera, T. F.; Kebarle, P. In *Ionic Processes in the Gas Phase*; Almoster Fereira, M., Ed.; NATO ASI Series 118; Reidel: Dordrecht, The Netherlands, 1984; p 135.
(68) Marcus, R. A. *J. Chem. Phys.* **1956**, *24*, 966.
(69) Drazaic, P. S.; Brauman, J. I. *J. Am. Chem. Soc.* **1982**, *104*, 13.
(70) Hay, P. J. *J. Chem. Phys.* **1982**, *76*, 502.
(71) Richardson, D. E. *J. Phys. Chem.* **1986**, *90*, 3697.
(72) Chowdhury, S.; Kebarle, P. *J. Chem. Phys.* **1986**, *90*, 4989.
(73) Jordan, K. D.; Burrow, P. D. *Acc. Chem. Res.* **1976**, *11*, 341. *J. Chem. Phys.* **1979**, *71*, 5384.
(74) Streitwieser, A., Jr. *Molecular Orbital Theory for Organic Chemists*; Wiley: New York, 1966; p 173.
(75) Fujio, M.; McIver, R. T.; Taft, R. W. *J. Am. Chem. Soc.* **1981**, *103*, 4017. Taft, R. W. *Prog. Phys. Org. Chem.* **1983**, *14*, 247.
(76) Birch, A. J.; Hinde, A. L.; Radom, L. *J. Am. Chem. Soc.* **1980**, *102*, 3310.
(77) Trumpower, B. L., Ed. *Function of Quinones in Energy Conserving Systems*; Academic: New York, 1982.
(78) Morton, R. A., Ed. *Biochemistry of Quinones*; Academic: New York, 1965.
(79) Parson, W. W. In *Photosynthetic Bacteria*; Clayton, R. K., Ed.; Academic: New York, 1975; p 445.
(80) Anand, N.; Bindra, J. S.; Ranganathan, S. *Art in Organic Synthesis*; Holden Day: San Francisco, 1970.
(81) Rozeboom, M. D.; Tegino-Larsen, I. S.; Horik, K. N. *J. Org. Chem.* **1981**, *46*, 2338.
(82) Heilbronner, E.; Bock, H. *Das HMO Model und Sciene Anwendung Grundlagen und Handhabung*; Verlag Chemie: Weinheim, FDR, 1968; p 345.
(83) Streitwieser, A. *Molecular Orbital Theory for Organic Chemistry*; Wiley: New York, 1966; p 289.
(84) Brauman, J. I.; Blair, L. K. *J. Am. Chem. Soc.* **1971**, *93*, 4315.
(85) Yamdagni, R.; Kebarle, P. *J. Am. Chem. Soc.* **1973**, *95*, 4050.
(86) Cooper, C. D.; Naff, W. T.; Compton, R. N. *J. Chem. Phys.* **1975**, *63*, 2752.
(87) Cooper, C. D.; Frey, W. F.; Compton, R. N. *J. Chem. Phys.* **1978**, *69*, 2367.
(88) Paul, G.; Chowdhury, S.; Kebarle, P. *J. Am. Chem. Soc.*, to be submitted for publication.
(89) Heibronner, E. *Molecular Spectroscopy*; Institute of Petroleum: London, 1976. Brundle, C. R.; Robin, M. B.; Kuebler, N. A. *J. Am. Chem. Soc.* **1972**, *94*, 1466.
(90) Burrow, P. D.; Michjeda, J. A.; Jordan, K. D. *J. Am. Chem. Soc.* **1976**, *98*, 6392. Jordan, K. D.; Michejda, J. A.; Burrow, P. D. *Ibid.* **1976**, *98*, 6392.
(91) Lifshitz, C. *J. Phys. Chem.* **1983**, *87*, 3474.
(92) Symons, C. R. M.; Selby, R. C.; Smith, I. G.; Bratt, S. W. *Chem. Phys. Lett.* **1977**, *48*, 100.
(93) Symons, M. C. R. *J. Chem. Soc., Faraday Trans. 2* **1981**, *77*, 783.
(94) Shchegoleva, L. N.; Bilkis, I. I.; Schastner, P. V. *Chem. Phys.* **1983**, *82*, 343.
(95) Christophorou, L. G. *Adv. Electron. Electron Phys.* **1978**, *56*, 55.
(96) Chen, C. L.; Chantry, P. J. *J. Chem. Phys.* **1979**, *71*, 3897.
(97) Su, T.; Bowers, M. T. *Int. J. Mass Spectrom. Ion Phys.* **1975**, *17*, 211.
(98) Herbst, E.; Patterson, T. A.; Lineberger, W. C. *J. Chem. Phys.* **1974**, *61*, 1300.
(99) Nalley, S. J.; Compton, R. N.; Schweinler, H. E.; Anderson, V. E. *J. Chem. Phys.* **1973**, *59*, 4125.
(100) Woo, S. B.; Helmy, E. M.; Mauk, P. H.; Paszek, A. P. *Phys. Rev. A* **1981**, *24*, 1380.
(101) Dunkin, D. B.; Fehsenfeld, F. C.; Ferguson, E. E. *Chem. Phys. Lett.* **1972**, *15*, 257.
(102) Rafaey, K. M. A. *J. Chem. Phys.* **1976**, *65*, 2002.
(103) Lefferet, C. B.; Jackson, W. M.; Rothe, E. W. *J. Chem. Phys.* **1973**, *58*, 5801. Lefferet, C. B.; Tang, S. Y.; Rothe, E. W.; Cheng, T. C. *J. Chem. Phys.* **1974**, *61*, 4929.
(104) Feldman, D. *Z. Naturforsch., A: Astrophys., Phys. Phys. Chem.* **1970**, *A25*, 621.
(105) Fefaey, K. M. A. *Int. J. Mass Spectrom. Ion Phys.* **1976**, *21*, 21.
(106) Hughes, B. M.; Lifshitz, C.; Tiernan, T. D. *J. Chem. Phys.* **1973**, *59*, 3162.
(107) Compton, R.; Reinhardt, P. W.; Cooper, C. D. *J. Chem. Phys.* **1978**, *68*, 4360. *Ibid.* **1978**, *68*, 2023.
(108) (a) Chen, E. C. M.; Wentworth, W. E. *J. Phys. Chem.* **1983**, *87*, 45. (b) Becker, R. S.; Chen, E. J. *J. Chem. Phys.* **1966**, *45*, 240. (c) Wentworth, W. E.; Chen, E.; Lovelock, J. E. *J. Phys. Chem.* **1966**, *70*, 495.
(109) Hirao, K. *J. Chem. Phys.* **1986**, *83*, 1433.
(110) Compton, R.; Reinhardt, P. W.; Cooper, C. D. *J. Chem. Phys.* **1975**, *63*, 3821. Compton, R.; Cooper, C. D. *J. Chem. Phys.* **1973**, *59*, 4140.
(111) Dispert, H.; Lachman, K. *Hahn-Meitner-Inst. Kernforsch. Berlin*, [*Ber.*] **1975**, *HMI-B 198*, 34.
(112) (a) Foster, R. *Organic Charge-Transfer Complexes*; Academic: New York, 1969. (b) Mashori, J. M.; Kochi, J. K. *J. Am. Chem. Soc.* **1985**, *107*, 6781.
(113) Stanley, J.; Smith, D.; Latimer, B.; Devlin, J. P. *J. Phys. Chem.* **1966**, *70*, 2011. Rettig, M. F.; Wing, M. *Inorg. Chem.* **1969**, *8*, 2685. Reiger, P. H.; Fraenkel, G. K. *J. Chem. Phys.* **1962**, *37*, 2795.
(114) Lyons, L. E.; Palmer, L. D. *Aust. J. Chem.* **1976**, *29*, 1919.
(115) Farragher, A. L.; Page, F. M. *Trans. Faraday Soc.* **1967**, *63*, 2369.
(116) Chen, E. C. M.; Wentworth, W. E. *J. Chem. Phys.* **1975**, *63*, 3186.
(117) Lindholm, E.; Asbrink, L. *Lect. Notes Chem.* **1985**, *35*, 206.
(118) Peover, M. E. *Trans. Faraday Soc.* **1962**, *58*, 1656.
(119) Matsen, F. A. *J. Chem. Phys.* **1956**, *24*, 602.
(120) Parker, V. D. *J. Am. Chem. Soc.* **1976**, *98*, 98.
(121) Dewar, M. J. S.; Hashmall, J. A.; Trinajstic, N. *J. Am. Chem. Soc.* **1970**, *92*, 5555.
(122) Magnera, T. F.; Caldwell, G.; Sunner, J.; Ikuta, S.; Kebarle, P. *J. Am. Chem. Soc.* **1984**, *106*, 6140.
(123) French, M. A.; Ikuta, S.; Kebarle, P. *Can. J. Chem.* **1982**, *60*, 1907.
(124) Chowdhury, S.; Kebarle, P., to be published.
(125) Terrier, F. *Chem. Rev.* **1982**, *82*, 77. Artamkina, G. A.; Egorov, M. P.; Belefskaya, I. P. *Ibid.* **1982**, *82*, 427.
(126) Hiraoka, K.; Mizuse, S.; Hamabe, S. *J. Chem. Phys.*, to be published (private communication).
(127) Sieck, L. W. *J. Phys. Chem.* **1985**, *89*, 5552.
(128) Chen, E. C.; Wentworth, W. E. *J. Phys. Chem.* **1983**, *87*, 45.
(129) Cooks, R. G.; Kruger, T. L. *J. Am. Chem. Soc.* **1977**, *99*, 1279.
(130) Puzo, G.; Prome, J. C. *Org. Mass Spectrom.* **1984**, *19*, 448.
(131) Harada, K.; Suzuki, M.; Kimbara, H. *Org. Mass Spectrom.* **1982**, *17*, 386.
(132) Sunner, J. A.; Kulatunga, R.; Kebarle, P. *Anal. Chem.* **1986**, *58*, 1312; **1986**, *58*, 2009.
(133) Sunner, J. A.; Morales, A.; Kebarle, P. *Anal. Chem.*, in press.
(134) Vestal, M. L. *Anal. Chem.* **1984**, *56*, 2590.
(135) Iribarne, J. V.; Thomson, B. A. *J. Chem. Phys.* **1976**, *64*, 2287. Banic, C. M.; Iribarne, J. V. *J. Chem. Phys.* **1985**, *83*, 6432.
(136) Alexander, A. J.; Kebarle, P. *Anal. Chem.* **1986**, *58*, 471.
(137) Hunt, D. F.; Crow, F. W. *Anal. Chem.* **1978**, *50*, 1781.
(138) Rose, M. E.; Johnstone, R. A. W. *Mass Spectrometry for Chemists and Biochemists*; Cambridge University: Cambridge, UK, 1982; p 96.
(139) Clayton, E.; Wakefield, J. C. *J. Chem. Soc., Chem. Commun.* **1984**, 969.
(140) Cotter, M. L.; Lloyd, J. R. *Proceedings of the 33rd Conference on Mass Spectrometry and Allied Topics*, San Diego, CA; American Society for Mass Spectrometry: East Lansing, MI, 1985; p 817.

(141) Barber, M. *J. Chem. Soc., Chem. Commun.* **1981**, 325.
(142) Bush, K. L.; Hass, J. R.; Bursey, M. M. *Org. Mass Spectrom.* **1978**, *13*, 604.
(143) Tannenbaum, H.; Roberts, J. D.; Dougherty, R. C. *Anal. Chem.* **1975**, *47*, 49.
(144) Bartmess, J. E.; Scott, J. A.; McIver, R. T. *J. Am. Chem. Soc.* **1979**, *101*, 6046.
(145) Cumming, J. B.; Kebarle, P. *Can. J. Chem.* **1978**, *56*, 1.
(146) Tiernan, T. O.; Chang, C. C. *EHP, Environ. Health Perspect.* **1980**, *36*, 47.